

***IN VIVO* PHOSPHORYLATION OF BACTERIAL-TYPE
PHOSPHOENOLPYRUVATE CARBOXYLASE FROM DEVELOPING
CASTOR OIL SEEDS AT THREONINE-4 AND SERINE-451**

by

Katie Jane Dalziel

A thesis submitted to the Department of Biology
in conformity with the requirements for
the degree of Master of Science

Queen's University
Kingston, Ontario, Canada
August 2011

Copyright © Katie J. Dalziel, 2011

Abstract

Phosphoenolpyruvate carboxylase (PEPC) is a tightly controlled anaplerotic enzyme situated at a pivotal branchpoint of plant C-metabolism. Plant genomes encode several closely related plant-type PEPC (PTPC) isozymes, and a distantly related bacterial-type PEPC (BTPC). Two physically and kinetically distinct oligomeric classes of PEPC occur in the endosperm of developing castor oil seeds (COS). Class-1 PEPC is a typical homotetramer composed of 107-kDa PTPC subunits, whereas the novel 910-kDa Class-2 PEPC hetero-octameric complex arises from a tight interaction between Class-1 PEPC and 118-kDa bacterial-type PEPC (BTPC) subunits. BTPC functions as a catalytic and regulatory subunit of the allosterically-desensitized Class-2 PEPC, hypothesized to support PEP-flux to malate for leucoplast fatty acid synthesis. Previous studies established that BTPC: (i) subunits of COS Class-2 PEPC are phosphorylated at multiple sites *in vivo* and (ii) phosphorylation at Ser⁴²⁵ provides a new tier of enzyme control in developing COS. LC MS/MS and LTQ-FT MS identified Thr⁴ and Ser⁴⁵¹ as additional *in vivo* phosphorylation sites of immunopurified COS BTPC (corresponding to acidophilic and basophilic protein kinase consensus sequences, respectively). Immunoblots probed with a phosphorylation-site specific antibody raised against a synthetic phosphopeptide indicated that Ser⁴⁵¹ phosphorylation is promoted during seed development, becoming maximal in stage VII (full cotyledon) COS. Although several pThr⁴ containing BTPC peptides were non-immunogenic, the collective results indicate that Thr⁴ is also phosphorylated *in vivo*. Kinetic effects of each phosphorylation site were examined using phospho-mimetic mutants of heterologously expressed COS BTPC. BTPC's phosphorylation at Ser⁴⁵¹ appears to be inhibitory, as reflected by significantly increased

$K_m(\text{PEP})$ values, and reduced $I_{50}(\text{malate})$ and $I_{50}(\text{Asp})$ values of a S451D mutant. By contrast, kinetic characterization of a T4D phosphomimetic mutant indicated that Thr⁴ phosphorylation is not regulatory in nature. However, Thr⁴ exists in a conserved forkhead-associated (FHA) binding domain (pTXXD) that has received considerable prominence as a phospho-Thr dependent protein interaction module. These results further our understanding of multisite phosphorylation of BTPC in developing COS and its possible contribution to the control of Class-2 PEPC activity.

Co-Authorship

With the exception of mass-spectrometry, all experimentation was performed within the Plaxton lab. Dr. Yimin She (previously, Dept. of Chemistry, Queen's University, currently Health Canada, Ottawa) oversaw all mass spectrometric experimentation. The work presented in Chapter 2 is representative of a few collaborators. Dr. Srinath Rao performed the cloning, mutagenesis and optimization of expression for all PEPC constructs. Brendan O'Leary performed the immunoblots pertaining to the characterization of the anti-pSer⁸⁷⁹ (Fig. 2.3), as well as all work done on characterization of the anti-pSer⁴²⁵ in (Figs. 2.3 and 2.6). Carlyne Brikis, an undergraduate thesis student, performed the initial dot blots and immunoblots pertaining to the characterization of the anti-pSer⁴⁵¹ in (Fig. 2.3 and 2.4 A).

Acknowledgements

First and foremost I would like to thank Dr. Plaxton for his continuing support throughout my time in the lab. Dr. Plaxton has been an excellent mentor, always striving for the best and inspiring me to do the same. I would also like to thank my committee members, Dr. Wayne Snedden and Dr. Graham Cote for their support throughout this process. Many thanks to past Plaxton lab members, Srinath Rao, Hue Tran for making the office an enjoyable place to work and Glen Uhrig for all his hard work and numerous co-IP samples that came in handy. Thanks to the present lab members, Whitney Robinson, Hernan Del Vecchio, Vicki Knowles, Joonho Park and Eric Fedosejevs for filling everyday and a lot of nights with laughs. I would like to specially thank Brendan O'Leary for all his guidance and support in and out of the lab, the journey would not have been as enjoyable without such a great mentor in the lab. Thank you to the Snedden lab, Kyle Bender and David Maj, for always providing entertaining lunch conversations, they will definitely be missed. To Jill Brenner and Joanne Berridge who have been there from the beginning, words cannot describe how thankful I am to have gone through this journey with two such amazing friends. Lastly, I would like to thank my family for their continued support, it is very much appreciated. I would not be where I am today without your continued encouragement.

Table of Contents

Abstract.....	ii
Co-Authorship.....	iv
Acknowledgements.....	v
Table of Contents.....	vi
List of Figures.....	viii
List of Tables.....	ix
List of Abbreviations.....	x
Chapter 1. Introduction and Literature Review.....	1
1.1 Physiological roles of PEPC.....	1
1.2 Carbon partitioning in developing seeds.....	2
1.3 Post-translational control of plant-type PEPC.....	4
Allosteric effectors.....	4
Regulatory phosphorylation.....	4
Monoubiquitination.....	6
1.4 Class-2 PEPC complexes.....	8
Discovery of the bacterial-type PEPC (BTPC) gene.....	8
Discovery of bacterial-type PEPC (BTPC) polypeptides.....	8
Tissue-specific expression of bacterial-type PEPC (BTPC) in castor plant.....	11
Post-translational modification of BTPC in castor oil seed.....	12
1.5 Thesis Objectives.....	13
Chapter 2. In vivo phosphorylation of bacterial-type phosphoenolpyruvate carboxylase from developing castor oil seeds in at Thr⁴ and Ser⁴⁵¹.....	21
2.1 Abstract.....	21
2.2 Introduction.....	22
2.3 Materials and Methods.....	25
Plant material.....	25
Co-immunopurification and protein phosphatase treatments.....	25
LC MS/MS analysis and phosphopeptide identification.....	25
Site-directed mutagenesis and heterologous expression of recombinant PEPCs.....	26
Purification of recombinant Class-2 PEPCs.....	27
Preparation of phosphosite specific antibodies against pThr ⁴ , pSer ⁴⁵¹ , and pSer ⁸⁷⁹ of COS BTPC.....	28

Electrophoresis and immunoblotting	29
Enzyme and protein assays and kinetic studies	29
Statistics	30
2.4 Results and Discussion	30
BTPC phosphosite mapping	30
Phospho-site specific antibodies confirm the phosphorylation of Ser ⁴⁵¹ in vivo.....	32
Monitoring Ser ⁴⁵¹ phosphorylation status throughout COS development and following COS depodding	34
Characterization of phosphomimetic mutants suggests that Ser ⁴⁵¹ phosphorylation inhibits BTPC within a Class-2 PEPC complex	35
2.5 Conclusion	39
Chapter 3. General Discussion	49
References.....	53
Appendix A. NetPhos phospho-site prediction score and phosphomimetic mutant purifications	61
Appendix B. Biological Replicates of in vivo phosphorylation status of Ser ⁴⁵¹ in developing COS endosperm	63

List of Figures

Figure 1.1 The phospho <i>enol</i> pyruvate carboxylase reaction.....	15
Figure 1.2 The diverse functions of plant PEPC.....	16
Figure 1.3 Models illustrating several metabolic functions of plant PEPC.....	17
Figure 1.4 Amino acid sequence alignment of <i>Arabidopsis</i> and castor oil plant PEPC isoenzymes.....	18
Figure 1.5 Model illustrating the biochemical complexity of castor bean PEPC.....	20
Figure 2.1 COS BTPC MS/MS analysis and phosphorylation site mapping.....	41
Figure 2.2 Partial alignment of COS BTPC Thr ⁴ and Ser ⁴⁵¹ domains with other vascular plant BTPCs.....	42
Figure 2.3 Specificity of phosphosite-specific antibodies.....	43
Figure 2.4 <i>In vivo</i> phosphorylation status of Ser ⁴⁵¹ in developing COS endosperm.....	44
Figure 2.5 Purification of recombinant Class-2 PEPC mutants.....	45
Figure 2.6 Sensitivity of recombinant Class-2 PEPC mutants to effectors.....	46
Figure 2.7 pH activity profile of recombinant Class-2 PEPC mutants	47

List of Tables

Table 2.1 PEP saturation kinetics of wild-type and phosphomimetic mutants of heterologously expressed Class-2 PEPC.....	48
-------------------------------------------------------------------------------------------------------------------------	----

List of Abbreviations

λ -P ^γ tase	lambda phosphatase
A ₂₈₀	absorbance at the 280 nanometer wavelength
BLAST	Basic Local Alignment Search Tool
BTPC	bacterial type phospho <i>enol</i> pyruvate carboxylase
CAM	Crassulacean acid metabolism
COS	castor oil seed
CBB-R250	Coomassie Brilliant Blue 250
Co-IP	co-immunopurification
DDL	dawdle protein
DTT	dithiothreitol
FT-ICR-MS	Fourier transform ion cyclotron resonance mass spectrometry
FHA	forkhead associated
FPLC	fast protein liquid chromatography
Glu-6-P	glucose-6-phosphate
Gly-3-P	glycerol-3-phosphate
HPLC	high performance liquid chromatography
I ₅₀	half maximal inhibition concentration
KAPP	kinase associated protein phosphatase
LC	liquid chromatography
MDH	malate dehydrogenase
MS	mass spectrometry
MS/MS	tandem mass spectrometry
NCBI	National Center for Biotechnology Information
OAA	oxaloacetate
PAGE	polyacrylamide gel electrophoresis
PEP	phospho <i>enol</i> pyruvate
PEPC	phospho <i>enol</i> pyruvate carboxylase
P _i	orthophosphate
PK _c	cytosolic pyruvate kinase

PK _p	plastidic pyruvate kinase
PP2A	protein phosphatase type 2A
PPCK	PEPC protein kinase
ProQ-PPS	Pro-Q Diamond Phosphoprotein stain
PTM	post-translational modification
qTOF	quadrupole time of flight
RT	retention time
SnRK1	sucrose non-fermenting related kinase
TCA	tricarboxylic acid cycle

Chapter 1. Introduction and Literature Review

Phosphoenolpyruvate (PEP) carboxylase (PEPC; E.C. 4.1.1.31) is a ubiquitous, and tightly controlled cytosolic enzyme found in vascular plants, green algae and bacteria. It catalyzes the irreversible β -carboxylation of phosphoenolpyruvate (PEP) in the presence of HCO_3^- to yield oxaloacetate (OAA) and P_i , using Mg^{2+} as a cofactor (Fig. 1.1)[1]. PEPC plays pivotal roles in photosynthetic CO_2 fixation by C_4 and Crassulacean acid metabolism (CAM) leaves, as well as in the anaplerotic replenishment of tricarboxylic acid (TCA) cycle intermediates that are withdrawn for biosynthesis and N-assimilation (Fig. 1.2)[1,2]. There are two distinct types of PEPC isozymes in vascular plant and green alga: plant-type PEPC (PTPC) that belongs to a small multi-gene family in vascular plants, and a distantly related bacterial-type PEPC (BTPC)[3-7]. The well studied Class-1 PEPCs usually exist as 400-440 kDa homotetramers, consisting of 4 identical 100-110 kDa PTPC subunits [2,8]. PTPCs have been categorized as being either photosynthetic [C_4 and CAM PEPCs] or non-photosynthetic (C_3) isozymes [9]. Vascular plant and algal BTPCs, however, physically interact with a Class-1 PEPC homotetramer to form the novel hetero-octamer Class-2 PEPC complex which is discussed below in detail [10-12]

1.1 Physiological roles of PEPC

Photosynthetic PTPC of C_4 and CAM leaves reduce photorespiration and function as a CO_2 concentrating mechanism to improve overall photosynthetic efficiency by up to 2-fold compared to C_3 leaves [13-16]. In addition, PEPC has a wide range of non-photosynthetic roles including supporting carbon–nitrogen interactions, seed formation

and germination, fruit ripening, guard cell metabolism during stomatal opening, and provision of malate as a respiratory substrate for symbiotic N₂-fixing bacteroids of legume root nodules (Fig. 1.2)[17]. The role of PEPC in the control of carbon partitioning in developing oil seeds is the focus of this thesis. PEP metabolism via PEPC and cytosolic pyruvate kinase (PK_c) and plastidic pyruvate kinase (PK_p) isozymes plays a key role in partitioning photosynthate to either leucoplast fatty acid biosynthesis or mitochondrial production of carbon skeletons and ATP needed for storage protein biosynthesis (Fig. 1.3) [17, 93].

1.2 Carbon partitioning in developing seeds

In developing seeds the partitioning of imported photosynthate between starch, storage lipid (triglycerides), and storage protein biosynthesis is of major agronomic concern. Developing seeds act as metabolic sinks that import sugars and amino acids from leaves and subsequently metabolize them into starch, triglycerides and storage proteins. Photosynthate may either be imported into the leucoplast for fatty acid biosynthesis or the mitochondria for production of C-skeletons and ATP needed for storage protein biosynthesis (Fig. 1.3). The partitioning of carbon between the leucoplast and mitochondria is largely dependent on PEP metabolism via PEPC, PK_c and PK_p [93]. In particular, PEPC activity and storage protein biosynthesis have been linked due to the requirement for OAA and 2-oxoglutarate (2-OG) to assimilate N during formation of amino acids [17-20]. Additional C skeletons are required when seeds import N in the form of amino acids because (i) glutamine, a major component of the supplied amino acids, contains two amino groups per 2-OG skeleton, and (ii) amino acids such as alanine can be deaminated and respired through the TCA cycle to yield NH₄⁺ that must be re-

assimilated into glutamine or glutamate via glutamine synthetase and glutamate-oxoglutarate amino transferase (GS/GOGAT) (Fig. 1.2A).

In addition PEPC has been shown to contribute to fatty acid synthesis through generation of metabolic precursors and reducing power. Fatty acid synthesis within the leucoplast is ATP and NAD(P)H dependent and uses acetyl-CoA as a precursor (Fig. 1.3B). The pathway from sucrose-derived cytosolic hexose-6Ps to plastidial acetyl-CoA is very flexible and varies within and between species (Fig. 1.3B) [21,22]. Studies of isolated leucoplasts from developing castor oil seed (COS) and *Helianthus annuus* (sunflower) seeds showed that exogenous malate, compared to other precursors, supported maximal rates of fatty acid synthesis [23,24]. When malate is oxidized into acetyl-CoA by plastidic NADP-ME and isozymes of pyruvate dehydrogenase complex (PDC) it produces all the reductant required for carbon incorporation into fatty acids [24]. In addition (i) storage lipid accumulation is closely related to PEPC and NADP-ME activity and protein abundance [7,10,25,26], and (ii) in castor cytosolic malate is transported into the leucoplast via a malate/Pi antiport of the leucoplast envelope [27]. Metabolic flux studies on non-green developing maize and sunflower embryos demonstrated 30% and 10% of carbon flux into fatty acids was derived from PEPC generated malate [28,29] adding to the evidence for PEPC's involvement in fatty acid synthesis in non green oil seeds. All of this evidence suggests that PEPC plays an important role in sucrose partitioning at the cytosolic PEP branchpoint to produce C-skeletons and reductant required for fatty acid biosynthesis in developing oil seeds such as COS (Fig. 1.3).

Pioneering work in the 1960's by Harry Beevers (Univ. of Purdue) and colleagues has led to the wide spread use of COS as a model system for studies in oilseed development and germination, carbon metabolism and triacylglyceride storage and mobilization. The castor genome was recently sequenced and annotated providing an important foundation for further investigation of regulatory and metabolic networks of castor-oil biosynthesis [30]. Additionally, COS contains more triacylglycerides than any other seed examined to date (~64% of total seed weight) [31,32].

1.3 Post-translational control of plant-type PEPC

PTPCs are controlled by allosteric effectors, as well as by a variety of post-translational modifications (PTMs).

Allosteric effectors

Allosteric control of Class-1 PEPC is accomplished through both feed-forward activation and feedback inhibition. Hexose- and triose-phosphates such as glucose-6-phosphate (Glu-6-P) and glycerol-3-phosphate (Gly-3-P) are activators of PEPC, whereas L-malate, L-aspartate, and L-glutamate are feedback inhibitors (Figs. 1.1 and 1.3A) [1,10,17,33,34].

Regulatory phosphorylation

Regulatory PEPC phosphorylation was initially discovered with C₄ and CAM photosynthetic Class-1 PEPCs [35]. Their PTPC subunits are phosphorylated on a highly conserved Ser residue close to the N-terminus of the protein (Fig. 1.4) [1,35]. Phosphorylation at this site decreases PEPC's sensitivity to allosteric inhibitors while increasing its affinity for PEP and allosteric activators [1,2,17,35,36]. A 30-33 kDa

calcium-independent PEPC protein kinase (PPCK) and protein phosphatase type 2A (PP2A) mediate the reversible phosphorylation of Class-1 PEPC [35-39]. PPCK is highly specific for the conserved N-terminal seryl phosphorylation site as it cannot phosphorylate N-terminal seryl mutant PEPCs [37,40,41]. Its high specificity may be due to the fact that PPCK lacks any regulatory domain and only contains a core kinase domain, making it the smallest protein kinase documented [2,36]. Class-1 PEPC phosphorylation appears to be largely controlled by changes in rates of PPCK synthesis and degradation, although allosteric effectors and dithiol-disulfide interconversion may also play a role [2,35,39].

Due to the lack of regulatory domains PPCK appears to be upregulated by a range of signals, including light in C₄ leaves, a circadian rhythm in CAM leaves, light and N supply in C₃ leaves, nutritional P_i deprivation in C₃ plants and cell cultures, and photosynthate supply in legume root nodules and developing castor seeds [35,36,39,42-47]. Studies with developing COS and soybean root nodules showed that endogenous PPCK activity, transcripts and PTPC subunit phosphorylation disappeared in response to prolonged darkness of intact plants. Reillumination of these plants resulted in recovery of PPCK activity and PTPC phosphorylation [39,48-50]. It is clear that regaining of photosynthate supply to these non-photosynthetic sink tissues provides a direct link between sucrose and the upregulation of PPCK and PTPC phosphorylation. In addition, studies on the PP2A involved in dephosphorylating PEPC have shown constant levels throughout plant tissues lending to the idea that PEPC phosphorylation is largely controlled by PPCK activity [1,51,52]. However, further research is needed to assess the

possibility that the activity of the PP2A catalytic subunits are controlled by its associated regulatory subunits.

Several post-translational PPCK controls have been proposed including (i) malate inhibition of PPCK activity, by potentially interacting with PEPC [38,39,53], (ii) dithiol-disulfide interconversion [39,41,54], and (iii) a proteinaceous inhibitor [55]. However, further studies are needed to confirm these mechanisms *in vivo*.

In addition to controlling enzymatic activity protein phosphorylation can provide docking sites for other proteins to mediate protein-protein interactions. One of the more common protein groups known to mediate protein-protein interactions through protein phosphorylation is the 14-3-3 family. They are a highly conserved and abundant protein family that plays a central role in eukaryotic cells [56]. 14-3-3s have been implicated as a binding partner of the PTPC isozyme AtPPC1 following tandem affinity purification of 14-3-3 complexes from transgenic *Arabidopsis* seedlings [57]. Despite this finding, AtPPC1 does not contain a known 14-3-3 binding motif and attempts to demonstrate 14-3-3 binding to purified phospho- and dephosphorylated forms of native AtPPC1 using far western overlay assays have been unsuccessful [58, W. Plaxton and C. Mackintosh, unpublished]. Additional research is needed to determine whether or not 14-3-3s do in fact bind to AtPPC1 and if they exert an influence on the kinetic or regulatory properties of AtPPC1 or other plant PEPCs.

Monoubiquitination

Ubiquitin is small, highly conserved globular protein found in eukaryotic cells. Ubiquitin can be covalently attached to a target protein through an isopeptide bond between the C-terminal Gly residue of ubiquitin and the ϵ -amino group of a Lys residue

on the target protein. The attachment of ubiquitin to its target protein is mediated by activating (E1), conjugating (E2) and ligating (E3) enzymes. Polyubiquitination is well known as a PTM that targets proteins for degradation by the 26S proteasome. PTPC and PPCK have both been suggested to be degraded by the polyubiquitination and proteasome pathway [59,60].

Conversely, monoubiquitination is a reversible PTM that mediates protein:protein interactions and protein localization and is involved in several processes such as endocytosis, DNA repair, transcription and translation, and signal transduction [61,62]. Interestingly, Class-1 PEPC purified from germinating COS endosperm was a heterotetramer containing a 1:1 ratio 110- and 107-kDa PTPC polypeptides. Several lines of evidence (N-terminal microsequencing, mass spectrometry (MS) and immunoblotting) showed that both polypeptides arise from the same PTPC gene (RcPpc3), but the 110-kDa subunit is a monoubiquitinated form of the 107-kDa subunit (Fig. 1.5). Lys-628 [63], a residue conserved in all PTPCs and BTPCs located proximal to a PEP binding/catalytic domain, was identified as PEPCs monoubiquitination site by MS/MS. Characterization of this PTM included incubating pure germinated COS Class-1 PEPC with a deubiquitinating enzyme [USP-2 (Ubiquitin specific protease-2) catalytic core] resulting in cleavage of ubiquitin from the 110-kDa subunit. This led to a reduction in the enzyme's $K_m(\text{PEP})$ and sensitivity to allosteric activators and inhibitors [63]. PTPC monoubiquitination has since been found in *Lilium longiflorum* (lily) pollen [6] and an immunoreactive doublet seen in germinating COS endosperm has also been observed on PTPC immunoblots from a broad variety of plants and tissues [64-67]. Additional

research is necessary to fully understand the prevalence and metabolic functions of PTPC monoubiquitination.

1.4 Class-2 PEPC complexes

The physical association of BTPC subunits with PTPC subunits to form Class-2 PEPC complexes (Fig. 1.5) adds to the already intricate regulation and modification of Class-1 PEPC.

Discovery of the bacterial-type PEPC (BTPC) gene

Annotation of *Arabidopsis* and rice genomes led to the discovery of a PEPC gene whose deduced amino acid sequence differed greatly from that of PTPCs [3]. In fact, these genes were more similar to those encoding PEPCs found in proteobacteria, and thus named BTPCs. BTPCs are thought to have evolved in green algae, and every sequenced plant genome contains at least one BTPC gene. Green algal BTPC genes encode an ~130 kDa polypeptide, whereas vascular plants BTPC genes encode polypeptides ranging from ~116 – 118 kDa [17].

Discovery of bacterial-type PEPC (BTPC) polypeptides

The discovery of BTPC polypeptides began in unicellular green algae (*Selenastrum minutum* and *Chlamydomonas reinhardtii*). Two distinct PEPC classes that exhibited different kinetic and physical properties but shared an identical PTPC subunit were purified and characterized [11,12,68-70]. These two classes were named Class-1 PEPC (consisting of a homotetramer of PTPC subunits) and Class-2 PEPC (high M_r complexes of Class-1 PEPC tightly associated with an immunologically unrelated 130-kDa subunit, subsequently shown to be BTPC). This novel Class-2 PEPC demonstrated

enhanced thermal stability, a broader pH-activity profile, biphasic PEP saturation kinetics and a greatly reduced sensitivity to allosteric effectors [11,12,69]. Algal BTPC appears to be phosphorylated on unknown residues which may be involved in BTPC:PTPC subunit stoichiometry within Class-2 PEPC [70]. Studies of BTPC have led to several characteristics that distinguish it from PTPCs. The main criteria are: (i) C-terminal tetrapeptide is (R/K)NTG for BTPCs or QNTG for PTPCs, (ii) BTPCs lack the N-terminal seryl phosphorylation motif (Acid-Base-XX-SIDAQLR) that PTPCs contain [3,5,7] and (iii) all BTPCs contain an intrinsically disordered region which consists of a 10-kDa insertion that is unstructured and highly flexible (Fig. 1.4) [71].

In 2003 Blonde and Plaxton [10] subsequently purified two distinct oligomeric classes of PEPCs from developing COS endosperm and found that their respective physical and kinetic/regulatory properties were extremely similar to those of Class-1 vs. Class-2 PEPCs of unicellular green algae. COS Class-1 PEPC was determined to be a 410-kDa homotetramer of 107-kDa PTPC subunits, whereas COS Class-2 PEPC exists as a 910-kDa hetero-octameric complex in which the Class-1 PEPC homotetrameric core is tightly associated with four 118-kDa BTPC subunits (Fig. 1.5) [7,10]. Similar to algal Class-2 PEPCs, the COS Class-2 PEPC complex exhibited a broader pH activity profile, decreased allosteric sensitivity and greater thermostability than Class-1 PEPC [10]. Furthermore, Class-1 and Class-2 PEPC showed unique developmental profiles in developing COS, in which Class-2 PEPC was found to be more abundant in earlier stages, peaking at stage V (maximal oil synthesis) whereas Class-1 increased throughout development and peaked at stage VII-IX (mature cotyledon) [7,10]. *In vitro* techniques such as co-immunopurification (co-IP), non-denaturing PAGE of clarified extracts

coupled with in-gel PEPC activity staining, and parallel immunoblotting using BTPC- and PTPC-specific antibodies have further documented the presence of Class-1 and Class-2 PEPCs in developing COS [7,48,72].

Unfortunately, native BTPC subunits of green algal and vascular plant Class-2 PEPCs are highly susceptible to rapid *in vitro* proteolytic cleavage [7,11,12]. This occurs at a specific site located within their intrinsically disordered region by an endogenous thiol endopeptidase. Some protection from proteolysis can be achieved with the use of phenylmethylsulfonyl fluoride and the ProteCEASE 100 Cocktail marketed by G-Biosciences, making clarified COS extracts suitable for immunoblotting and co-IP of non-degraded BTPC [7,72]. This high susceptibility to proteolysis has been a major issue in studying native BTPC from developing COS endosperm. To overcome this obstacle, highly enriched native BTPC from developing COS endosperm was co-IP'd using an anti-(castor PTPC)-IgG immunoaffinity column [72]. A second approach was to purify recombinant COS BTPC (RcPPC4) from *Escherichia coli* cells in which it has been heterologously expressed. This approach was not ideal as purified RcPPC4 readily formed aggregates that tended to precipitate. However, by titrating purified RcPPC4 aggregate into recombinant *Arabidopsis* PTPC (AtPPC3), an active chimeric Class-2 PEPC was readily formed [73]. With this knowledge *E. coli* lysates containing wild-type versions of castor BTPC (RcPPC4) were mixed with lysates containing the *Arabidopsis* PTPC (AtPPC3) to create intact, stable chimeric Class-2 PEPCs *in vitro*, which were then purified and characterized [73]. This technique then allowed for analysis of: i) the kinetic properties of the BTPC subunits, ii) the regulatory effect of the BTPC subunits exert on PTPC subunits within a Class-2 PEPC, and iii) the effects of phosphomimetic mutations

on the kinetic and regulatory properties of BTPC subunits [71,73]. Several lines of evidence strongly suggest that BTPC does not exist on its own *in vivo*, but rather needs PTPC in order to form a stable Class-2 complex. For example (i) native BTPCs have only been seen in association with PTPC subunits in a Class-2 complex, (ii) BTPC subunits tightly associate with PTPC subunits during purification, (iii) heterologously expressed BTPC forms aggregates in *E. coli* lysates in the absence of PTPC subunits, and (iv) fluorescent protein-tagged COS BTPC subunits interact *in vivo* via its disordered region with COS PTPC during their transient co-expression in tobacco BY2 cells [6,7, 10-12, 17, 74].

Tissue-specific expression of bacterial-type PEPC (BTPC) in castor plant

Although most studies have focused on BTPC expression as a Class-2 PEPC subunit in the endosperm of developing COS, a recent study has expanded the search for BTPC to other tissues in the castor plant (*Ricinus communis*) [67]. The results of this study demonstrate that BTPC transcripts and polypeptides: (i) are abundant in inner integument, cotyledon and endosperm of developing COS but occur at low levels in roots and cotyledons of germinated COS, and (ii) show a unique developmental profile pattern in leaves such that they are present in leaf buds and young expanding leaves, but undetectable in fully expanded leaves [67]. Class-2 PEPC and its BTPC subunits therefore appear to be a characteristic feature of rapidly growing tissues that require a large anaplerotic flux from PEP to replenish TCA cycle intermediates consumed during biosynthesis.

Post-translational modification of BTPC in castor oil seed

In addition to COS BTPC acting as a catalytic and regulatory subunit in Class-2 PEPC, it is also subject to multisite *in vivo* phosphorylation (Fig. 1.5)[72]. Preliminary experiments with the phospho-protein stain Pro-Q Diamond revealed that co-IP'd BTPC from developing COS is highly phosphorylated *in vivo* [72]. In addition, P_i-affinity PAGE using Phos-Tag acrylamide in conjunction with λ-p³tase treatment demonstrated that COS BTPC is phosphorylated at multiple sites [72]. MS/MS was then used to determine one of the specific phosphorylation sites, Ser⁴²⁵ [71, 72]. In addition to this site a potential phosphorylation site (Ser⁸⁷⁹) was proposed due to its presence in a precise recognition motif for by plant SNF-1 protein related kinase 1 (SnRK1) (Fig. 1.4) [72]. This motif requires hydrophobic residues at positions -5 and +4 and basic residues at -3 and -6 and is conserved in vascular plant BTPCs.

The discovery of Class-2 PEPCs and their PTPC and BTPC subunits in developing COS have led to a better understanding of BTPCs biochemical and functional properties. Recent studies on the phosphorylation at Ser⁴²⁵ in developing COS have given some insight BTPC's role in Class-2 PEPC. However, further studies are required to elicit more about its physiological functions [71].

Phospho-site specific antibodies were crucial for studying Ser⁴²⁵ phosphorylation of COS BTPC *in vivo* [71]. These antibodies were made by immunizing a rabbit with a short phosphopeptide corresponding to the sequence surrounding the phospho-site. A developing COS endosperm profile of BTPC's pSer⁴²⁵ content demonstrated that phosphorylation increased from stage III – IX, coinciding with oil production. Removal of sucrose supply by depodding, induced a rapid increase in COS BTPC

Ser⁴²⁵ phosphorylation [71]. This differs from COS PTPC that demonstrated a rapid decrease in phosphorylation with removal of photosynthate, leading to the conclusion that PTPC phosphorylation at Ser¹¹ and BTPC phosphorylation at Ser⁴²⁵ are controlled by different protein kinases and phosphatases. Lastly, BTPC's pSer⁴²⁵ content appears to have a slight diel cycle where phosphorylation increases during the day compared to PTPC where Ser¹¹ phosphorylation status does not change with regard to diurnal cycles [71].

Phosphomimetic mutants (Ser to Asp) were a second crucial tool used in studying the regulatory effects of phosphorylating COS BTPC at Ser⁴²⁵ [71]. It should be noted that although Class-2 PEPC was used for these studies, its PTPC subunits were inactive mutants (AtPPC3_R644A) so only kinetics of BTPC would be observed. The introduction of an Asp at residue 425 increased COS BTPC K_m (PEP) ~4 fold and lowered its I_{50} (Asp and Mal) values by ~2.5 fold compared to wildtype dephosphorylated BTPC. These results indicated that COS BTPC is subject to regulatory inhibition when phosphorylated at Ser⁴²⁵ [71].

1.5 Thesis Objectives

Previous studies indicated that BTPC is subject to multi-site phosphorylation in developing COS [72]. However, only one site (Ser⁴²⁵) has been mapped and studied in detail [71,72]. The objectives for my MSc thesis research were to: (i) map any additional *in vivo* phosphorylation sites of COS BTPC using MS, (ii) raise phospho-site specific antibodies to each site, (iii) use these antibodies to determine the influence of COS development and depodding on BTPC site-specific phosphorylation profiles, and (iv) deduce kinetic effect of each *in vivo* phosphorylation site using phospho-mimetic mutants

of heterologously expressed COS BTPC. It is hypothesized that *in vivo* multi-site phosphorylation of Class-2 PEPC's BTPC subunits plays an important role in the control of C-partitioning to storage end-products in developing COS.

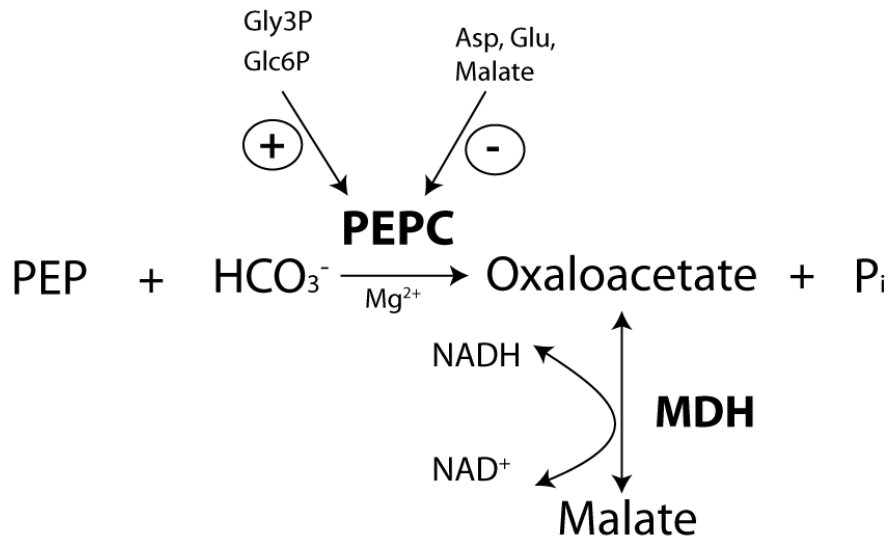


Figure 1.1: The phosphoenolpyruvate carboxylase reaction The conversion of PEP to oxaloacetate releasing P_i requires the presence of HCO_3^- and the metal cofactor Mg^{2+} . Glycerol-3-phosphate and glucose-6-phosphate act as allosteric activators whereas aspartate, glutamate, and malate act as allosteric inhibitors.

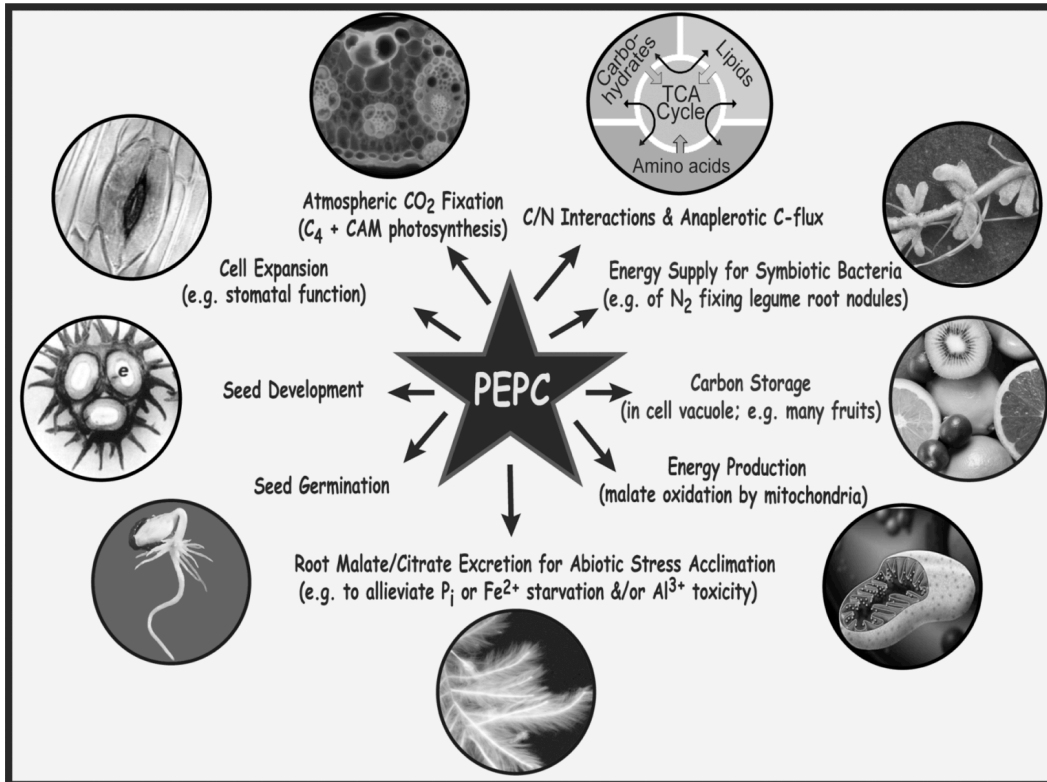


Figure 1.2 The diverse functions of plant PEPC. PEPC has a variety of functions including: CO₂ fixation in C₄ and CAM plants, C/N interactions, anaplerotic replenishment, N₂ fixation, carbon storage, energy production, abiotic stress acclimation, seed germination, seed development, and cell expansion (Taken from [17]).

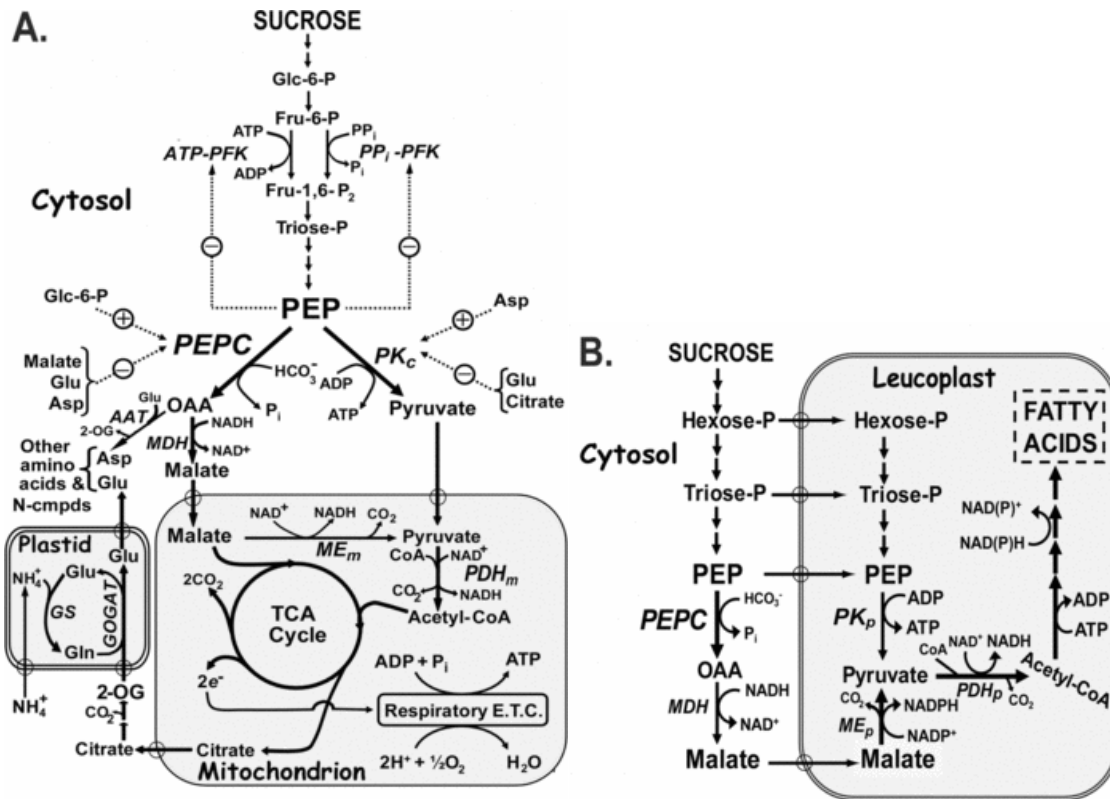


Figure 1.3 Models illustrating several metabolic functions of plant PEPC. (A) Interactions between carbon and nitrogen metabolism involves three compartments in plant cells. This scheme highlights the important role of the two terminal enzymes of plant cytosolic glycolysis, PEPC and PK_c, in controlling the provision of the mitochondria with respiratory substrates, as well as for generating the 2-OG and OAA respectively required for NH₄⁺-assimilation via GS/GOGAT in plastids and aspartate amino transferase in the cytosol. The co-ordinate control of PEPC and PK_c by allosteric effectors, particularly glutamate and aspartate, provides a mechanism for the regulation of cytosolic glycolytic flux and PEP partitioning during and following NH₄⁺-assimilation. **(B)** This model illustrates the role of PEPC in controlling PEP partitioning to malate as a source of carbon skeletons and reducing power for leucoplast fatty acid synthesis. Abbreviations are as defined in the text, in addition to the following: AAT, Asp aminotransferase; E.T.C., electron transport chain; ME_m/PDH_m and ME_p/PDH_p, mitochondrial and plastidic isoenzymes of ME and PDH respectively (Taken from [17]).

RcPPC1 MAGRNVLVIMASIDAQLRLLALRKSVEEDKLVEDALLDRFLDILQDLHGEDI--RETVCYCELSAEYEGKHNPKLAE--LQKVLTSLDPGDSIVVTKSFHMLNLANLAEVEQIAYRR 117
 RcPPC3 MQPRNLEKLA¹IDAQLRLLVPAKVSSEDDKLVEDALLDRFLDILQDLHGEDI--RETVCYCELSAEYEGKHDPKLE--LGNLLTSLD²PGDSIVIAKSFHMLNLANLAEVEQIAYRR 117
 AtPPC1 MANRLEKMA³IDVHLRQLVPGKVSSEDDKLVEDALLDRFLDILQDLHGEDI--RETVCYELHSAEYEGKHEPKLEE--LGSVLTSLD⁴PGDSIVIAKAFSHMLNLANLAEVEQIAYRR 117
 AtPPC3 MARRNLEKMASIDAQLRQLVPAKVSSEDDKLVEDALLDRFLDILQDLHGEDI--REFVQELYELSAEYEGKREPKLEE--LGSVLTSLD⁵PGDSIVISKAFSHMLNLANLAEVEQIAYRR 117
 AtPPC2 MAARNLEKMASIDAQLRQLVPAKVSSEDDKLVEDALLDRFLDILQDLHGEDI--REFVQELYELSAEYEGKREPKLEE--LGNMLTSLD⁶PGDSIVVTKSFHMLNLANLAEVEQIAYRR 117
 RcPPC4 -----MTD⁷TDIAEIEISFQSFEDDKLLG--SLFHDVLQREVGNPFMEKVERIRILAQSALNRLMAGIEDTANLEKQLEISRMTELEALTLARAFSHYLNMGIAETHRRH-- 109
 AtPPC4 -----MTD⁸TDIAEIEISFQSFEDDKLLG--SLFHDVLQREVGNPFMEKVERIRILAQSALNRLMAGIEDTANLEKQLEISRMTELEALTLARAFSHYLNMGIAETHRRH-- 109

I

RcPPC1 RIK-LKKGFADENSATTSDEIETLKRLLVQLKSPPEEVFDALKNQTV¹VDVLT²TAHPT³OSVRRSLQKHARIRDCLTQLYAKDITPDDKQELDEALQREIQA⁴AFRTDEIRRTPT⁵QDEM 236
 RcPPC3 RNK-LKKGFADENSATTSDEIETLKRLLVQLKSPPEEVFDALKNQTV⁶VDVLT⁷TAHPT⁸OSVRRSLQKHARIRDCLTQLYAKDITPDDKQELDEALQREIQA⁹AFRTDEIRRTPT¹⁰QDEM 236
 AtPPC1 RIKLKKGFVDESSATTSDEIETLKRLLVQLKSPPEEVFDALKNQTV¹¹VDVLT¹²TAHPT¹³OSVRRSLQKHARIRDCLTQLYAKDITPDDKQELDEALQREIQA¹⁴AFRTDEIRRTPT¹⁵QDEM 237
 AtPPC3 RIKLKKGFVDESSATTSDEIETLKRLLVQLKSPPEEVFDALKNQTV¹⁶VDVLT¹⁷TAHPT¹⁸OSVRRSLQKHARIRDCLTQLYAKDITPDDKQELDEALQREIQA¹⁹AFRTDEIRRTPT²⁰QDEM 237
 AtPPC2 RIKLKKGFADENSATTSDEIETLKRLLVQLKSPPEEVFDALKNQTV²¹VDVLT²²TAHPT²³OSVRRSLQKHARIRDCLTQLYAKDITPDDKQELDEALQREIQA²⁴AFRTDEIRRTPT²⁵QDEM 236
 RcPPC4 -----KARSMHLKSCDDIFNQLLSGSI²⁶SAEELYD²⁷YVCKQ²⁸VEV²⁹LVLT³⁰TAHPT³¹OSVRRSLQKHARIRDCLTQLYAKDITPDDKQELDEALQREIQA³²AFRTDEIRRTPT³³QDEM 218
 AtPPC4 -----KVHWVQLARSCDDIFNQLLSGSI³⁴SAEELYD³⁵YVCKQ³⁶VEV³⁷LVLT³⁸TAHPT³⁹OSVRRSLQKHARIRDCLTQLYAKDITPDDKQELDEALQREIQA⁴⁰AFRTDEIRRTPT⁴¹QDEM 218

RcPPC1 RAGSYFHETIWKGVKPKFLRRVD¹TALKNIGINERVPYNAPL²IQ³SSW⁴GGDR⁵GNPRV⁶TEV⁷TRD⁸VCLLAR⁹MAANLY¹⁰FSQ¹¹IEDL¹²MF¹³SM¹⁴WR¹⁵CNE----- 332
 RcPPC3 RAGSYFHETIWKGVKPKFLRRVD¹⁶TALKNIGINERVPYNAPL¹⁷IQ¹⁸SSW¹⁹GGDR²⁰GNPRV²¹TEV²²TRD²³VCLLAR²⁴MAANLY²⁵FSQ²⁶IEDL²⁷MF²⁸SM²⁹WR³⁰CSD----- 332
 AtPPC1 RAGSYFHETIWKGVKPKFLRRVD³¹TALKNIGINERVPYNAPL³²IQ³³SSW³⁴GGDR³⁵GNPRV³⁶TEV³⁷TRD³⁸VCLLAR³⁹MAATMY⁴⁰FNQ⁴¹IEDL⁴²MF⁴³SM⁴⁴WR⁴⁵CND----- 333
 AtPPC3 RAGSYFHETIWKGVKPKFLRRVD⁴⁶TALKNIGINERVPYNAPL⁴⁷IQ⁴⁸SSW⁴⁹GGDR⁵⁰GNPRV⁵¹TEV⁵²TRD⁵³VCLLAR⁵⁴MAANLY⁵⁵FNQ⁵⁶IEDL⁵⁷MF⁵⁸SM⁵⁹WR⁶⁰CTD----- 333
 AtPPC2 RAGSYFHETIWKGVKPKFLRRVD⁶¹TALKNIGINERVPYNAPL⁶²IQ⁶³SSW⁶⁴GGDR⁶⁵GNPRV⁶⁶TEV⁶⁷TRD⁶⁸VCLLAR⁶⁹MAANLY⁷⁰FSQ⁷¹IEDL⁷²MF⁷³SM⁷⁴WR⁷⁵CNE----- 332
 RcPPC4 RAGLNV⁷⁶EQSL⁷⁷WKAL⁷⁸PHYL⁷⁹RRV⁸⁰S⁸¹TALK⁸²KH--TGKPL⁸³PL⁸⁴CT⁸⁵TP⁸⁶RF⁸⁷GS⁸⁸W⁸⁹GGDR⁹⁰GNPN⁹¹TA⁹²KT⁹³TRD⁹⁴VCLLAR⁹⁵MA⁹⁶VDLY⁹⁷I⁹⁸RE⁹⁹VD¹⁰⁰SL¹⁰¹RF¹⁰²EL¹⁰³SM¹⁰⁴VQ¹⁰⁵CS¹⁰⁶RL¹⁰⁷LK¹⁰⁸VAND¹⁰⁹IL¹¹⁰EET¹¹¹SS¹¹²ED¹¹³HES¹¹⁴WN 337
 AtPPC4 RAGLNV¹¹⁵EQSL¹¹⁶WKAV¹¹⁷QYL¹¹⁸RRV¹¹⁹S¹²⁰TALK¹²¹KF--TGKPL¹²²PL¹²³CT¹²⁴TP¹²⁵RF¹²⁶GS¹²⁷W¹²⁸GGDR¹²⁹GNPN¹³⁰TA¹³¹KT¹³²TRD¹³³VCLLAR¹³⁴MA¹³⁵VDLY¹³⁶I¹³⁷RE¹³⁸VD¹³⁹SL¹⁴⁰RF¹⁴¹EL¹⁴²ST¹⁴³DR¹⁴⁴CS¹⁴⁵RL¹⁴⁶FS¹⁴⁷RL¹⁴⁸AD¹⁴⁹K¹⁵⁰LE¹⁵¹KD-----YD 338

RcPPC1 -----ELR¹VRADEL-----HRTSR²KDA--KH³YIEFWK⁴QI 359
 RcPPC3 -----ELR⁵VRADEL-----HR⁶SKR⁷DS--KH⁸YIEFWK⁹QV 359
 AtPPC1 -----ELR¹⁰ARADEV-----HAN¹¹SR¹²KDA¹³AK¹⁴HYIEFWK¹⁵SI 361
 AtPPC3 -----EFR¹⁶VRADEL-----HR¹⁷NSR¹⁸KDA¹⁹AK²⁰HYIEFWK²¹TI 361
 AtPPC2 -----ELR²²VRAER-----OR²³CAK²⁴DA--KH²⁵YIEFWK²⁶LI 358
 RcPPC4 QPASRS²⁷Q²⁸TK²⁹F³⁰PK³¹SL³²PT³³QL³⁴PPA³⁵DL³⁶PA³⁷CT³⁸EC³⁹ND⁴⁰GES⁴¹Q⁴²Y⁴³PK⁴⁴LE⁴⁵PG⁴⁶TD⁴⁷Y⁴⁸MP⁴⁹FN⁵⁰R⁵¹Q⁵²EAL⁵³SS⁵⁴Y⁵⁵ESS⁵⁶SS⁵⁷QD⁵⁸IN⁵⁹H⁶⁰GL⁶¹PK⁶²TT⁶³GN⁶⁴GS⁶⁵VAN⁶⁶SS⁶⁷GS⁶⁸PR⁶⁹AF⁷⁰SS--AQ⁷¹LV⁷²AQ⁷³RK⁷⁴LA⁷⁵ES⁷⁶SG⁷⁷SK⁷⁸Q⁷⁹KL 456
 AtPPC4 R⁸⁰GS⁸¹N⁸²F⁸³Q⁸⁴Q⁸⁵SS⁸⁶CL⁸⁷PT⁸⁸QL⁸⁹PARA⁹⁰HL⁹¹PA⁹²CI⁹³DF--GES⁹⁴R⁹⁵HT⁹⁶K⁹⁷FE⁹⁸I⁹⁹AT¹⁰⁰TD¹⁰¹Y¹⁰²MP¹⁰³N¹⁰⁴Q¹⁰⁵NE¹⁰⁶Q¹⁰⁷DES¹⁰⁸WE¹⁰⁹K¹¹⁰IND¹¹¹GS-----R¹¹²SL¹¹³TS¹¹⁴RG¹¹⁵S¹¹⁶TS¹¹⁷QL¹¹⁸L¹¹⁹QR¹²⁰K¹²¹FE¹²²ES¹²³Q¹²⁴Y¹²⁵KT¹²⁶SK¹²⁷QL 436

X

RcPPC1 PPS-----EPY¹RV²LD³GV⁴DR⁵DK⁶LY⁷NR⁸TR⁹SR¹⁰QL¹¹LANG¹²ISDI¹³PEE¹⁴AT¹⁵FN¹⁶VE¹⁷Q¹⁸FL¹⁹EP²⁰LE²¹PL²²CY²³SL²⁴CAC²⁵GR²⁶PI²⁷AD²⁸GS²⁹LL³⁰DF³¹LR³²QV³³ST³⁴FG³⁵LS³⁶VR³⁷LD³⁸IR³⁹QES⁴⁰ER⁴¹HT⁴²VD⁴³LD⁴⁴IT⁴⁵K⁴⁶HL⁴⁷IG⁴⁸-F 471
 RcPPC3 PPS-----EPY⁴⁹RV⁵⁰LD⁵¹GD⁵²RV⁵³DK⁵⁴LY⁵⁵NR⁵⁶TR⁵⁷SR⁵⁸QL⁵⁹SH⁶⁰NS⁶¹DI⁶²PEE⁶³AT⁶⁴FN⁶⁵VE⁶⁶Q⁶⁷FL⁶⁸EP⁶⁹LE⁷⁰PL⁷¹CY⁷²SL⁷³CSC⁷⁴GD⁷⁵PI⁷⁶AD⁷⁷GS⁷⁸LL⁷⁹DF⁸⁰LR⁸¹QV⁸²ST⁸³FG⁸⁴LS⁸⁵VR⁸⁶LD⁸⁷IR⁸⁸QES⁸⁹ER⁹⁰HT⁹¹VD⁹²LD⁹³IT⁹⁴K⁹⁵HL⁹⁶IG⁹⁷-S 471
 AtPPC1 PPT-----EPY⁹⁸RV⁹⁹LD¹⁰⁰GD¹⁰¹VR¹⁰²DK¹⁰³LY¹⁰⁴NR¹⁰⁵TR¹⁰⁶SR¹⁰⁷QL¹⁰⁸SH¹⁰⁹NS¹¹⁰DI¹¹¹PEE¹¹²AT¹¹³FN¹¹⁴VE¹¹⁵Q¹¹⁶FL¹¹⁷EP¹¹⁸LE¹¹⁹PL¹²⁰CY¹²¹SL¹²²CSC¹²³GD¹²⁴PI¹²⁵AD¹²⁶GS¹²⁷LL¹²⁸DF¹²⁹LR¹³⁰QV¹³¹ST¹³²FG¹³³LS¹³⁴VR¹³⁵LD¹³⁶IR¹³⁷QES¹³⁸ER¹³⁹HT¹⁴⁰VD¹⁴¹LD¹⁴²IT¹⁴³K¹⁴⁴HL¹⁴⁵IG¹⁴⁶-S 473
 AtPPC3 PPT-----EPY¹⁴⁷RV¹⁴⁸LD¹⁴⁹GD¹⁵⁰VR¹⁵¹DK¹⁵²LY¹⁵³NR¹⁵⁴TR¹⁵⁵SR¹⁵⁶QL¹⁵⁷SH¹⁵⁸NS¹⁵⁹DI¹⁶⁰PEE¹⁶¹AT¹⁶²FN¹⁶³VE¹⁶⁴Q¹⁶⁵FL¹⁶⁶EP¹⁶⁷LE¹⁶⁸PL¹⁶⁹CY¹⁷⁰SL¹⁷¹CSC¹⁷²GD¹⁷³PI¹⁷⁴AD¹⁷⁵GS¹⁷⁶LL¹⁷⁷DF¹⁷⁸LR¹⁷⁹QV¹⁸⁰ST¹⁸¹FG¹⁸²LS¹⁸³VR¹⁸⁴LD¹⁸⁵IR¹⁸⁶QES¹⁸⁷ER¹⁸⁸HT¹⁸⁹VD¹⁹⁰LD¹⁹¹IT¹⁹²K¹⁹³HL¹⁹⁴IG¹⁹⁵-S 474
 AtPPC2 PAN-----EPY¹⁹⁶RV¹⁹⁷LD¹⁹⁸GD¹⁹⁹VR²⁰⁰DK²⁰¹LY²⁰²NR²⁰³TR²⁰⁴SR²⁰⁵QL²⁰⁶SH²⁰⁷NS²⁰⁸DI²⁰⁹PEE²¹⁰AT²¹¹FN²¹²VE²¹³Q²¹⁴FL²¹⁵EP²¹⁶LE²¹⁷PL²¹⁸CY²¹⁹SL²²⁰CSC²²¹GD²²²PI²²³AD²²⁴GS²²⁵LL²²⁶DF²²⁷LR²²⁸QV²²⁹ST²³⁰FG²³¹LS²³²VR²³³LD²³⁴IR²³⁵QES²³⁶ER²³⁷HT²³⁸VD²³⁹LD²⁴⁰IT²⁴¹K²⁴²HL²⁴³IG²⁴⁴-S 470
 RcPPC4 [EP²⁴⁵PL²⁴⁶QR²⁴⁷PG²⁴⁸]PY²⁴⁹RV²⁵⁰LD²⁵¹GV²⁵²DK²⁵³LY²⁵⁴NR²⁵⁵TR²⁵⁶SR²⁵⁷QL²⁵⁸LE²⁵⁹LL²⁶⁰ED²⁶¹LP²⁶²CE²⁶³YD²⁶⁴QW²⁶⁵YE²⁶⁶TD²⁶⁷QL²⁶⁸DE²⁶⁹LL²⁷⁰PL²⁷¹CY²⁷²SL²⁷³Q²⁷⁴CG²⁷⁵AG²⁷⁶VL²⁷⁷AD²⁷⁸GR²⁷⁹LAD²⁸⁰L²⁸¹IR²⁸²RV²⁸³AT²⁸⁴FG²⁸⁵VL²⁸⁶KL²⁸⁷LD²⁸⁸QES²⁸⁹GR²⁹⁰HAD²⁹¹TD²⁹²IT²⁹³K²⁹⁴YL²⁹⁵MG²⁹⁶-T 575
 AtPPC4 [EP²⁹⁷PL²⁹⁸K²⁹⁹R³⁰⁰AG³⁰¹S]PY³⁰²RV³⁰³LD³⁰⁴GV³⁰⁵DK³⁰⁶LY³⁰⁷NR³⁰⁸TR³⁰⁹SR³¹⁰QL³¹¹LE³¹²LL³¹³EG³¹⁴LP³¹⁵CE³¹⁶YD³¹⁷P³¹⁸K³¹⁹NS³²⁰YE³²¹TS³²²D³²³QL³²⁴DE³²⁵LL³²⁶PL³²⁷CY³²⁸SL³²⁹Q³³⁰CG³³¹AG³³²VL³³³AD³³⁴GR³³⁵LAD³³⁶L³³⁷IR³³⁸RV³³⁹AT³⁴⁰FG³⁴¹VL³⁴²KL³⁴³LD³⁴⁴QES³⁴⁵AR³⁴⁶HS³⁴⁷LD³⁴⁸IT³⁴⁹TA³⁵⁰VL³⁵¹MG³⁵²-T 555

RcPPC1 YREWSE¹EH²RQ³EW⁴LL⁵TEL⁶R⁷K⁸RP⁹L¹⁰FP¹¹GD¹²L¹³P¹⁴KT¹⁵DE¹⁶IA¹⁷VD¹⁸TF¹⁹H²⁰IA²¹E²²L²³PAD²⁴FN²⁵GA²⁶Y²⁷IS²⁸MA²⁹TAP³⁰SD³¹VLA³²VEL³³LQ³⁴RE³⁵CV³⁶KQ³⁷P-----LR³⁸VV³⁹PL⁴⁰FE⁴¹K⁴²L⁴³AD⁴⁴LE⁴⁵AP⁴⁶AA⁴⁷VAR⁴⁸L⁴⁹FS⁵⁰IDW 580
 RcPPC3 YREWSE⁵¹EH⁵²RQ⁵³EW⁵⁴LL⁵⁵SEL⁵⁶SG⁵⁷K⁵⁸RP⁵⁹L⁶⁰FP⁶¹GD⁶²L⁶³Q⁶⁴RT⁶⁵DE⁶⁶VA⁶⁷VD⁶⁸TF⁶⁹H⁷⁰IA⁷¹E⁷²L⁷³PAD⁷⁴FN⁷⁵GA⁷⁶Y⁷⁷IS⁷⁸MA⁷⁹TAP⁸⁰SD⁸¹VLA⁸²VEL⁸³LQ⁸⁴RE⁸⁵CV⁸⁶KQ⁸⁷P-----LR⁸⁸VV⁸⁹PL⁹⁰FE⁹¹K⁹²L⁹³AD⁹⁴LE⁹⁵AP⁹⁶AA⁹⁷VAR⁹⁸L⁹⁹FS¹⁰⁰IDW 580
 AtPPC1 YREWSE¹⁰¹EH¹⁰²RQ¹⁰³EW¹⁰⁴LL¹⁰⁵SEL¹⁰⁶SG¹⁰⁷K¹⁰⁸RP¹⁰⁹L¹¹⁰FP¹¹¹GD¹¹²L¹¹³P¹¹⁴KT¹¹⁵DE¹¹⁶IA¹¹⁷VD¹¹⁸TF¹¹⁹H¹²⁰IA¹²¹E¹²²L¹²³PAD¹²⁴FN¹²⁵GA¹²⁶Y¹²⁷IS¹²⁸MA¹²⁹TAP¹³⁰SD¹³¹VLA¹³²VEL¹³³LQ¹³⁴RE¹³⁵CV¹³⁶KQ¹³⁷P-----LR¹³⁸VV¹³⁹PL¹⁴⁰FE¹⁴¹K¹⁴²L¹⁴³AD¹⁴⁴LE¹⁴⁵AP¹⁴⁶AA¹⁴⁷VAR¹⁴⁸L¹⁴⁹FS¹⁵⁰IDW 582
 AtPPC3 YR¹⁵¹DSE¹⁵²EG¹⁵³RQ¹⁵⁴EW¹⁵⁵LL¹⁵⁶SEL¹⁵⁷SG¹⁵⁸K¹⁵⁹RP¹⁶⁰L¹⁶¹FP¹⁶²GD¹⁶³L¹⁶⁴P¹⁶⁵KT¹⁶⁶EE¹⁶⁷IS¹⁶⁸VD¹⁶⁹TF¹⁷⁰H¹⁷¹IA¹⁷²E¹⁷³L¹⁷⁴PAD¹⁷⁵FN¹⁷⁶GA¹⁷⁷Y¹⁷⁸IS¹⁷⁹MA¹⁸⁰TAP¹⁸¹SD¹⁸²VLA¹⁸³VEL¹⁸⁴LQ¹⁸⁵RE¹⁸⁶CV¹⁸⁷KNP-----LR¹⁸⁸VV¹⁸⁹PL¹⁹⁰FE¹⁹¹K¹⁹²L¹⁹³AD¹⁹⁴LE¹⁹⁵AP¹⁹⁶AA¹⁹⁷VAR¹⁹⁸L¹⁹⁹FS²⁰⁰IDW 583
 AtPPC2 YK²⁰¹MS²⁰²ED²⁰³K²⁰⁴RQ²⁰⁵EW²⁰⁶LL²⁰⁷SEL²⁰⁸SG²⁰⁹K²¹⁰RP²¹¹LP²¹²GD²¹³L²¹⁴P²¹⁵KT²¹⁶EE²¹⁷VA²¹⁸VD²¹⁹TF²²⁰H²²¹IA²²²E²²³L²²⁴PAD²²⁵FN²²⁶GA²²⁷Y²²⁸IS²²⁹MA²³⁰TAP²³¹SD²³²VLA²³³VEL²³⁴LQ²³⁵RE²³⁶CV²³⁷ITDP-----LR²³⁸VV²³⁹PL²⁴⁰FE²⁴¹K²⁴²L²⁴³AD²⁴⁴LE²⁴⁵AP²⁴⁶AA²⁴⁷VAR²⁴⁸L²⁴⁹FS²⁵⁰IEW 579
 RcPPC4 YSE²⁵¹WDE²⁵²E²⁵³K²⁵⁴LE²⁵⁵FL²⁵⁶TR²⁵⁷EL²⁵⁸K²⁵⁹RP²⁶⁰LP²⁶¹VP²⁶²TE²⁶³VA²⁶⁴PD²⁶⁵VE²⁶⁶LD²⁶⁷AF²⁶⁸RV²⁶⁹AA²⁷⁰EL²⁷¹SG²⁷²DS²⁷³LG²⁷⁴AY²⁷⁵IS²⁷⁶MA²⁷⁷SN²⁷⁸AS²⁷⁹DV²⁸⁰LA²⁸¹VEL²⁸²LQ²⁸³DA²⁸⁴RL²⁸⁵AV²⁸⁶SEL²⁸⁷GR²⁸⁸PC²⁸⁹GG²⁹⁰TL²⁹¹RV²⁹²PL²⁹³FE²⁹⁴TV²⁹⁵N²⁹⁶DL²⁹⁷R²⁹⁸AG²⁹⁹GS³⁰⁰VI³⁰¹R³⁰²KL³⁰³LS³⁰⁴IDW 695
 AtPPC4 YSE³⁰⁵WDE³⁰⁶E³⁰⁷K³⁰⁸LE³⁰⁹FL³¹⁰TR³¹¹EL³¹²K³¹³RP³¹⁴LP³¹⁵VQ³¹⁶CI³¹⁷VG³¹⁸PD³¹⁹VE³²⁰LD³²¹AF³²²RV³²³AA³²⁴EL³²⁵SG³²⁶DS³²⁷LG³²⁸AY³²⁹IS³³⁰MA³³¹SN³³²AS³³³DV³³⁴LA³³⁵VEL³³⁶LQ³³⁷DA³³⁸RL³³⁹AV³⁴⁰SEL³⁴¹GR³⁴²PC³⁴³GG³⁴⁴TL³⁴⁵RV³⁴⁶PL³⁴⁷FE³⁴⁸TV³⁴⁹N³⁵⁰DL³⁵¹R³⁵²AG³⁵³GS³⁵⁴VI³⁵⁵R³⁵⁶KL³⁵⁷LS³⁵⁸IDW 675

II

III

RcPPC1 YRNRIN---GK¹QEV²MI³YSD⁴SG⁵DK⁶AGR⁷LSA⁸AQ⁹W¹⁰L¹¹YKA¹²QEL¹³V¹⁴KV¹⁵AK¹⁶YGV¹⁷KL¹⁸TF¹⁹H²⁰RG²¹GT²²VR²³GG²⁴GP²⁵TH²⁶L²⁷AIL²⁸S²⁹Q³⁰PP³¹DT³²I³³HS³⁴LR³⁵VT³⁶VQ³⁷GE³⁸VI³⁹EQ⁴⁰S⁴¹GE⁴²EH⁴³CF⁴⁴RT⁴⁵L⁴⁶Q⁴⁷TA⁴⁸TL⁴⁹EH⁵⁰ 696
 RcPPC3 YRNRIN---GK⁵¹QEV⁵²MI⁵³YSD⁵⁴

Figure 1.4 Amino acid sequence alignment of *Arabidopsis* and castor oil plant PEPC isoenzymes. Identified *in vivo* phosphorylation sites of castor and *Arabidopsis* PTPCs (RcPPC3 and AtPPC1 respectively) and castor BTPC (RcPPC4), are highlighted in green, as well as the predicted BTPC (RcPPC4) Ser⁸⁷⁹ phosphorylation site. RcPPC3's conserved Lys⁶²⁸ monoubiquitination site is marked with a red font. BTPC's intrinsically disordered region is enclosed in a red rectangle. The *in vitro* proteolytic cleavage site (Lys 446) of RcPPC4 is marked with an X. Boxes I–III denote conserved subdomains essential for PEPC catalysis. The predicted pI, molecular mass and sequence identity (%) of the various PEPCs are shown. The deduced PEPC sequences were aligned using ClustalW software (<http://www.ebi.ac.uk/Tools/clustalw2/index.html>). Colons and asterisks indicate conserved and identical amino acids, respectively (Adapted from [17]).

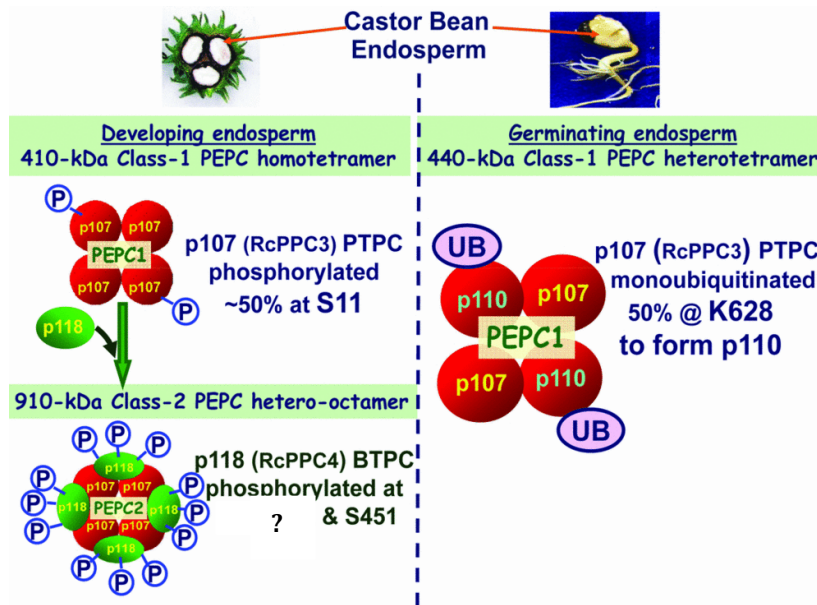


Figure 1.5 Model illustrating the biochemical complexity of castor bean PEPC

In developing COS endosperm the PTPC RcPPC3 (p107) exists as a Class-1 PEPC homotetramer (PEPC1) which is *in vivo* phosphorylated at Ser¹¹. In addition it associates with BTPC RcPPC4 subunits (p118) to form the novel heterooctameric Class-2 PEPC. The BTPC subunit is also subject to multisite phosphorylation at Ser⁴²⁵ as well as other unidentified residues [72,73]. Finally, in germinating COS Class-1 PEPC (RcPPC3) is monoubiquitinated at Lys 628 (Adapted from [17]).

Chapter 2. *In vivo* phosphorylation of bacterial-type phosphoenolpyruvate carboxylase from developing castor oil seeds in at Thr⁴ and Ser⁴⁵¹

K.J. Dalziel, B. O’Leary, Y-M. She, S.K. Rao, C. Brikis and W.C. Plaxton (2011)
Manuscript in preparation

2.1 Abstract

PEPC [PEP (phosphoenolpyruvate) carboxylase] is a tightly controlled anaplerotic enzyme situated at a pivotal branch point of plant carbohydrate-metabolism. Two distinct oligomeric PEPC classes were discovered in developing castor oil seeds (COS): Class-1 PEPC is a typical homotetramer of 107-kDa plant-type PEPC (PTPC) subunits, whereas the novel 910-kDa Class-2 PEPC hetero-octamer arises from a tight interaction between Class-1 PEPC and 118-kDa bacterial-type PEPC (BTPC) subunits. Mass spectrometric analysis of immunopurified COS BTPC indicated that it is subject to *in vivo* phosphorylation at Ser⁴²⁵, Ser⁴⁵¹ and Thr⁴. In addition a potential phosphorylation site (Ser⁸⁷⁹) was predicted due to its presence in the known plant SNF1-related protein kinase 1 (SnRK1) phosphorylation motif. Here, immunoblots probed with phosphorylation site-specific antibodies demonstrated that Ser⁴⁵¹ phosphorylation is promoted during seed development, becoming maximal in stage VII. COS Ser⁸⁷⁹ does not appear to be an *in vivo* phosphorylation site. Several synthetic pThr⁴ containing phosphopeptides were non-immunogenic. Kinetic analyses of a heterologously expressed chimeric Class-2 PEPC containing phosphomimetic BTPC mutant subunits (S451D) indicated that Ser⁴⁵¹ phosphorylation caused significant BTPC inhibition by: (i) increasing its $K_m(\text{PEP})$ three-fold, (ii) reducing its $I_{50}(\text{L-malate and L-Asp})$ values by 2-fold, respectively, while (iii) decreasing its activity within the physiological pH range. By contrast recombinant Class-2 PEPC containing a Thr⁴ phosphomimetic BTPC mutation did not show any difference

in $K_m(\text{PEP})$, sensitivity to effectors or activity with varying pH compared to wild-type BTPC. A double phosphomimetic mutant of Ser⁴²⁵ and Ser⁴⁵¹ (S425D+S451D) indicated that phosphorylation at both sites caused an intermediate level of BTPC inhibition. Collectively the results establish that BTPC's pSer⁴⁵¹ content depends upon COS developmental and physiological status and that Ser⁴⁵¹ phosphorylation significantly attenuates the catalytic activity of BTPC subunits within a Class-2 PEPC complex. This study, along with a previous study on regulatory BTPC phosphorylation at Ser⁴²⁵, provides further evidence of protein phosphorylation as a mechanism for the *in vivo* control of BTPC subunits of vascular plant Class-2 PEPC complexes.

2.2 Introduction

PEPC [PEP (phospho*enol*pyruvate) carboxylase] (EC 4.1.1.31) is a tightly regulated cytosolic enzyme of vascular plants and green algae that catalyzes the irreversible β -carboxylation of PEP in the presence of HCO_3^- to yield oxaloacetate and P_i . PEPC has been extensively studied with regards to its crucial role in catalyzing atmospheric CO_2 fixation in C_4 and CAM photosynthesis [1,2]. However, PEPC's essential non-photosynthetic functions, particularly the anaplerotic replenishment of tricarboxylic-acid-cycle intermediates consumed during biosynthesis and N-assimilation, have received increased attention within the last decade [17].

Plant PEPCs belong to a small multigene family encoding several plant-type PEPC (PTPC) genes, along with at least one distantly related bacterial-type PEPC (BTPC) gene [3,5,7]. PTPC genes encode closely related 100-110-kDa polypeptides that: (i) contain a conserved N-terminal seryl-phosphorylation domain and critical C-terminal tetrapeptide QNTG, and (ii) typically exist in a homotetramer known as Class-1 PEPC

[2,8,75]. Plant BTPC genes encode 116-118-kDa polypeptides exhibiting low (<40%) sequence identity with PTPCs and that contain a prokaryotic-like (R/K)NTG C-terminal tetrapeptide [17]. BTPC genes and transcripts were discovered in rice and *Arabidopsis* in 2003 [3]. They have since been well documented in several vascular plants, but a clear expression pattern has not yet emerged [3,4,6,7,76-78]. Insights into the structure, function and location of BTPC polypeptides began earlier with their discovery in unicellular green algae [5,11,12,69,70,79], and have continued with their subsequent discovery in developing castor bean endosperm [10] and most recently in developing lily pollen [6]. Examination of PEPC from these algal and vascular plant sources revealed the presence of a high- M_r Class-2 PEPC heteromeric complex composed of tightly associated PTPC and BTPC subunits that is remarkably desensitized to allosteric effectors relative to the corresponding Class-1 PEPCs [5,10-12]. Several lines of evidence strongly suggest that BTPCs only exist *in vivo* as part of a Class-2 PEPC complex [5,72,73].

Owing to its location at a pivotal branch point in primary carbon metabolism the activity of PEPC is tightly controlled *in vivo*. PTPCs have long been known to be controlled by a combination of allosteric effectors and reversible phosphorylation at their conserved N-terminal seryl residue catalyzed by a dedicated Ca^{2+} -independent PTPC protein kinase and PP2A (protein phosphatase type-2A) [1,2,56]. Phosphorylation at this site enhances allosteric activation by hexose-phosphates while reducing inhibition by L-malate and L-Asp. Manipulation of these control properties can cause drastic effects on carbon and nitrogen metabolism within the cell [17]. Recently, a number of other mechanisms for the post translational control of PEPC, including the formation of Class-

2 complexes, have emerged. Class-1 PEPC is also subject to inhibitory monoubiquitination at a conserved Lys residue during COS (castor oil seed; *Ricinus communis*) germination, causing an increased $K_m(\text{PEP})$ and enhanced sensitivity to allosteric effectors [63]. A chloroplast-targeted Class-1 PEPC isozyme exists in rice leaves, although the degree to which this phenomenon occurs in other plant species remains to be determined [80]. In developing castor endosperm BTPC and PTPC subunits associate into allosterically insensitive Class-2 PEPCs. Lastly, BTPC subunits from developing castor endosperm are phosphorylated at multiple sites *in vivo* [72]. Only one of these sites has been identified (Ser⁴²⁵), and it appears to cause inhibition of the BTPC subunits by increasing their $K_m(\text{PEP})$ and sensitivity to feedback inhibition [73].

The aim of the current study was to continue to elucidate the control properties of castor endosperm BTPC by identifying and characterizing its remaining phosphorylation sites. High sensitivity fourier transform mass spectrometry (FT-MS) was used to identify Thr⁴ and Ser⁸⁷⁹ as additional phosphorylation sites. Phosphosite-specific antibodies were then raised against these sites to confirm their existence and monitor their *in vivo* phosphorylation status. Lastly, phosphomimetic mutants of the Thr⁴ and Ser⁴⁵¹ phosphorylation sites were created to analyze the kinetic effects of phosphorylation at these sites. The combined results suggest that pSer⁴⁵¹ is an additional regulatory phosphorylation site of COS BTPC, whereas pThr⁴ forms part of a phosphothreonine-dependent protein interaction domain known as a forkhead-associated (FHA) domain.

2.3 Materials and Methods

Plant material

Castor bean plants (*Ricinus communis*; cv. Baker 296) were cultivated in a greenhouse at 24 °C and 70% humidity under natural light supplemented with 16 h of artificial light. Pods containing COS at various developmental stages were harvested at midday unless otherwise indicated. For depodding experiments, stems containing intact pods of developing COS were excised and placed in water in the dark at 24 °C. Developing endosperm and cotyledon tissues were rapidly dissected, frozen in liquid N₂, and stored at -80°C.

Co-immunopurification and protein phosphatase treatments

Co-IP of BTPC polypeptides from developing COS extracts using an anti-(COS PTPC) immunoaffinity column was conducted as previously described [72]. Enrichment of BTPC polypeptides was achieved using 100 mM glycine pH 2.8 to elute bound BTPC from the co-IP column. Incubation of co-IP samples with exogenous λ-phosphatase (New England BioLabs) was as previously described [48,72].

LC MS/MS analysis and phosphopeptide identification

Proteins were reduced with 10 mM dithiothreitol (DTT), alkylated with 55 mM iodoacetamide and dialyzed against 10 mM ammonium bicarbonate. Following tryptic digestion, the protein digest was dissolved in 0.2% formic acid (FA) for LC MS/MS analysis on either the Nano-Acquity ultra-performance liquid chromatography system (UPLC, Waters, Milford, MA) coupled to a 7-tesla hybrid linear ion-trap Fourier transform ion cyclotron resonance mass spectrometer (LTQ-FT ICR, Thermo Fisher) or

the Agilent 1100 capillary HPLC system coupled to a QStar XL quadrupole time-of-flight instrument (QqTOF, AB Sciex). The peptides were trapped and subsequently separated by a C18 analytical column of 1.7 μm BEH130 (100 μm x 100 mm, UPLC, Waters) or 3 μm PepMap 100 (75 μm x 150 mm, HPLC, LC packings) through a 90 min gradient from 5% to 30% of solvent B (acetonitrile containing 0.1% FA), then 85% at a flow rate of 0.5 $\mu\text{l}/\text{min}$. Automated data dependent acquisition was employed to obtain MS and MS/MS measurements at a mass range of m/z 300-2000. Dynamic exclusion was enabled for a period of 180 s.

Phosphopeptide identification was performed using an in-house Mascot Server (version 2.3.0, Matrix Science), and the data were searched against the National Center for Biotechnology Information (NCBI) database for *viridiplantae* (green plants). The parameter settings allowed trypsin digestion for maximum 2 missed cleavage sites, and a fixed peptide modification of cysteine carbamidomethylation. Deamidation of asparagine and glutamine, methionine oxidation, phosphorylation of serine, threonine and tyrosine were considered as variable modifications. Mass tolerances were set up to 10 ppm for the FT MS ions and 1 Da for ion trap MS/MS fragment ions, 100ppm for the QqTOF MS and 0.1 Da for MS/MS measurements. Phosphorylation sites were validated by manual inspection of MS/MS spectra with predicted fragments.

Site-directed mutagenesis and heterologous expression of recombinant PEPCs

Full-length cDNAs for AtPPC3 (PTPC isozyme from *Arabidopsis thaliana*) and RcPPC4 (BTPC isozyme from castor plant) were cloned into a pET28b His-tag vector (Novagen) and transformed into *E. coli* (BL21-CodonPlus (DE3)-RIL) (Stratagene) and heterologously expressed as previously described [71,73]. All AtPPC3 constructs used

encoded inactive (R644A) mutants as per [71]. The Quickchange II Site-Directed mutagenesis kit (Stratagene) was used to generate the desired mutant AtPPC3 construct (R644A) and RcPPC4 constructs (S451D, T4D and S451D+S425D) as per previously described [71]. Oligonucleotide primer pairs used to introduce the mutations were as follows, forward 5'GAATCCAAGATAGGAAGATCTGATTTCCAGAAACTTCTA-3' and reverse 5'-CTAGAAGTTTCTGGAAATCAGATCTTCCTATCTTGGATT-3' and for T4D forward 5'-GCCATATGACGGACGACACAGATGATATCGC-3' and reverse 5'-GCGATATCATCTGTGTGTCGTCATATGGC-3'; underlined is an introduced EcoRV restriction site. The double mutant (S425D+S451D) was created by further mutagenesis of the S425D plasmid [71] with the S451D primers. The amplified vectors were transformed into *E. coli* using electroporation and positive clones selected on LB plates containing 50 µg/ml kanamycin were further screened for the desired mutation by restriction digestion and sequencing. The PEPC coding portion in each plasmid from the confirmed clones was sequence verified.

Purification of recombinant Class-2 PEPCs

All purifications were conducted as previously described [71,73]. Briefly, *E. coli* cells containing the heterologously expressed RcPPC4 or the inactive AtPPC3 were lysed by passage through a French press and then mixed together. The resulting Class-2 PEPCs were purified using PrepEaseTM His-Tagged High Yield Purification Ni²⁺-affinity resin (USB Corp.) followed by Superdex-200 and Superpose-6 gel filtration FPLC (GE Biosciences). Pooled peak fractions were concentrated with an Amicon Ultra-15 centrifugal filter unit (100-kDa cut-off), frozen in liquid N₂, and stored at -80 °C. The

PEPC activity of the preparations were stable for at least 2 months when stored under these conditions.

Preparation of phosphosite specific antibodies against pThr⁴, pSer⁴⁵¹, and pSer⁸⁷⁹ of COS BTPC

Synthetic phospho- and dephospho-peptides were made corresponding to the regions around the putative Thr⁴, Ser⁴⁵¹ and putative Ser⁸⁷⁹ phosphorylation sites of COS BTPC with an additional cysteine at the N- terminus (Ser⁴⁵¹ and Ser⁸⁷⁹) or C-terminus (Thr⁴) by the Sheldon Biotechnology Centre, McGill University, Montreal QC, Canada (Fig. 2.3). Purified phosphopeptide (1 mg) was coupled to maleimide-activated keyhole limpet haemocyanin (Pierce Chemicals) according to the manufacturer's protocols. C-terminus coupling with an additional cysteine was attempted for a pThr⁴ containing phosphopeptide but was non immunogenic so a second coupling strategy was attempted. A new pThr⁴ peptide containing a pair of lysine residues at its C-terminus (Fig. 2.3) was coupled to both bovine serum albumin (BSA)(Pierce) and keyhole limpet haemocyanin with 2.5% (v/v) glutaraldehyde. pThr⁴ peptide was dissolved at 10 mg/ml in PBS at pH 7.4. The dissolved peptide (250 µl) was then mixed with either 1000 µl of 10 mg/ml each of KLH and BSA and 25 µl of 2.5 % (v/v) glutaraldehyde. A 0.5 h time point was taken for both the KLH and BSA conjugates (400 µl) and mixed with 50 µl of 1 M Tris (pH 7.5) to quench excess glutaraldehyde. The remaining peptide-glutaraldehyde mixture was left at room temperature for several hours until the reaction turned yellow and then mixed with 100 µl of 1M Tris pH 7.5. All four mixtures (BSA coupled (0.5 h and end point) and KLH coupled (0.5 h and end point) were mixed together. For both coupling strategies the conjugates were desalted into phosphate buffered saline via Sephadex G-25 gel

filtration FPLC (GE Healthcare), filter sterilized, and emulsified with Titermax Gold adjuvant (CytRx Corp.). Following collection of pre-immune serum, 500 µg of phosphopeptide conjugate was injected subcutaneously into a 2-kg New Zealand rabbit. A 250 µg booster injection was administered 30 d later. Seven days after the final injection, blood was collected in Vacutainer tubes (Becton Dickinson) by cardiac puncture, and the immune serum frozen in liquid N₂ and stored at -80 °C. For immunoblotting, anti-pSer⁴⁵¹ and anti-pSer⁸⁷⁹ immunoglobulin G was affinity-purified as previously described [48] using 500 µg of the corresponding synthetic phosphopeptide bound to nitrocellulose.

Electrophoresis and immunoblotting

SDS- and P_i-affinity-PAGE using a Bio-Rad Protean III minigel system were conducted as previously described [10]. For immunoblotting, minigels were electroblotted onto poly(vinylidene difluoride (PVDF) membranes and probed using antibodies described in the relevant figure legends. Antigenic polypeptides were visualized using an alkaline phosphatase-conjugated secondary antibody and chromogenic detection [81]. Rabbit anti-BTPC [anti-(COS BTPC)-IgG] was raised against homogeneous recombinant RcPPC4 as described previously [73]. All immunoblot results were replicated a minimum of three times with representative results shown in the various figures.

Enzyme and protein assays and kinetic studies

PEPC activity was assayed at 25 °C by following NADH oxidation at 340 nm using a kinetics microplate reader (Molecular Devices) and the following optimized 200-µl assay mixture: 50 mM Hepes/KOH (pH 8.0) containing 10% (v/v) glycerol, 10 mM PEP, 5 mM KHCO₃, 10 mM MgCl₂, 2 mM dithiothreitol, 0.15 mM NADH and 5 units•ml⁻¹ of porcine

muscle L-malate dehydrogenase (Roche). One unit of PEPC is defined as the amount of PEPC resulting in the production of 1 μmol of oxaloacetate $\cdot\text{min}^{-1}$. PEP saturation kinetic data for Class-2 PEPCs were fitted to a single active site model using nonlinear regression analysis software and apparent I_{50} values (inhibitor concentration producing 50% inhibition of PEPC activity) were calculated using a nonlinear least-square regression computer program [82]. All kinetic parameters represent means of at least four independent experiments and are reproducible to within $\pm 15\%$ S.E.M. of the mean value. Metabolite stock solutions were made equimolar with MgCl_2 and adjusted to pH 7.0. Protein concentrations were determined by the Coomassie Blue G-250 dye-binding using bovine γ -globulin as the protein standard [10].

Statistics

Data were analyzed using the Student's *t*-test, and deemed significant if $p < 0.02$

2.4 Results and Discussion

BTPC phosphosite mapping

Previous work has conclusively shown that a 118-kDa BTPC subunit is phosphorylated at multiple sites during COS development [72]. Both LC MS/MS and immunoblotting using anti-pSer⁴²⁵ specific antibodies identified Ser⁴²⁵ as an *in vivo* COS BTPC phosphorylation site [71,72]. Here, increased resolution and sensitivity afforded by the FT-ICR and QqTOF MS analysis of co-IP'd COS BTPC (93.4% sequence coverage) has independently verified the Ser⁴²⁵ phosphorylation site while identifying two additional sites, corresponding to Thr⁴ and Ser⁴⁵¹ (Fig. 2.1). Two abundant phosphopeptides were identified by FT-ICR-MS in which the intensity of peptide

corresponding to residues 447-454 at m/z 501.7430 (RT 14.61 min) was approximately three fold higher than that of the peptide corresponding to residues 413-427 at m/z 736.3142 (RT 11.41 min) (Fig. 2.1A). Fragmentation of the doubly charged ion of m/z 501.74 displayed an apparent loss of phosphoric acid (-49 m/z) resulting in a major fragment ion at 452.99. Analysis of the N-terminal b_n and C-terminal y_n ion series presented a 69 Da mass difference between two high-intensity fragments of y_3 and y_{4-18} . This corresponds to an abnormal dehydroalanine residue at Ser⁴⁵¹ which results from the loss of a P_i group from serine (Fig. 2.1B). The MS/MS spectrum of the precursor ion at m/z 736.31 unambiguously identified this phosphorylation site as the previously established pSer⁴²⁵ (Fig. 2.1C) [71,73]. Similar LC MS/MS was performed by QqTOF mass spectrometry, and identified a large phosphorylated peptide corresponding to residues 2-34 at m/z 970.95 (RT 30.11 min, Fig. 2.1D). Manual inspection of the data set indicated this low-abundance peptide had a charge state of 4+ (Fig. 2.1E). The collision induced dissociation of this quadruple charged ion generated a set of C-terminal y_n fragments ($n=1-12$) in the MS/MS spectrum and identified a spacing of 83 Da at b_2 indicating an abnormal dehydroaminobutyric acid residue caused by dephosphorylation of Thr⁴ (Fig. 2.1F).

Thr⁴ appears to exist in an FHA binding domain and also correspond to an acidic protein kinase recognition motif (Fig. 2.2). FHA domains are present in a wide variety of proteins and have gained considerable prominence as phospho-Thr dependent binding modules. Two prominent FHA binding motifs described so far are pTXXD and pTXXI/L/V [83]. The former motif occurs at the N-terminus of BTPC. By contrast, Ser⁴⁵¹ corresponds to a basophilic kinase motif having an arginine residue located at the -2

position (Fig. 2.2). Most basophilic kinases prefer substrates with basic residues in close proximity to the phosphorylated residue commonly at either the -2 or -3 position [84]. The location of Ser⁴⁵¹ is also of interest because secondary structure analysis using the Phyre server [85] predicted that this region of COS BTPC exists in a largely coiled, unstructured, and highly flexible conformation known as an intrinsically disordered region [71]. Disordered region containing proteins are ubiquitous to all organisms. Disordered regions typically exist as a flexible linker that freely twist and rotate through space to mediate protein:protein interactions [86]. PTMs such as proteolysis and phosphorylation at residues within disordered regions are common due to their high surface accessibility [86]. In this case, the COS BTPC disordered region also contains the Ser⁴²⁵ phosphorylation site, and the known BTPC proteolysis site at Lys⁴⁴⁶ [7,71]. Both Thr⁴ and Ser⁴⁵¹ are conserved in almost all other orthologous plant BTPC protein sequences deduced to date. The apparent exceptions are a substitution and deletion of Thr⁴ in *Glycine max* and *Mimulus guttatus* respectively, although these could represent errors in sequencing (Fig. 2.2).

Phospho-site specific antibodies confirm the phosphorylation of Ser⁴⁵¹ in vivo

Phospho-site specific antibodies have proven to be essential tools for confirming and studying the specific *in vivo* phosphorylation of proteins, especially those containing multiple phosphorylation sites [71]. To further analyze the phosphorylation status of COS BTPC, a series of phosphosite-specific antibodies were made corresponding to identified and putative BTPC phosphorylation sites. Antibodies were successfully raised against synthetic phosphopeptides corresponding to the sequences around pSer⁴⁵¹ and putatively phosphorylated Ser⁸⁷⁹ (Fig. 2.3). The Ser⁸⁷⁹ site was included as it was

previously suggested to be a potential phosphorylation site due to its presence in a well characterized plant SNF1-related protein kinase 1 (SnRK1) phosphorylation motif that appears to be conserved in other plant BTPC orthologs [72]. Each of the phospho-site specific antibodies was specific for the phosphorylated version of the corresponding synthetic peptide. The cross-reaction between the antibodies and the phosphopeptides was abolished when the antibody was pre-incubated with corresponding blocking phosphopeptide, whereas the addition of corresponding non-phosphorylated blocking peptide did not quench the cross-reaction (Fig. 2.3). The use of these blocking peptides alongside the inclusion of non-phosphorylated BTPC control lanes served to verify the specificity of these phosphosite-specific antibodies in subsequent immunoblots. Unfortunately, several different peptides corresponding to the Thr⁴ phosphorylation site were non-immunogenic as they failed to cross react with the corresponding phosphopeptide (Fig. 2.3A and 2.3B).

To verify and/or establish the presence of *in vivo* phosphorylation sites, co-IP'd native BTPC from stage VII developing COS endosperm was probed with each of the phosphosite-specific antibodies. Immunoblots with anti-pSer⁴⁵¹ specifically detected the 118 kDa BTPC polypeptide (p118) and this signal was eliminated by λ -phosphatase pre-treatment of the sample or by incubation with blocking phosphopeptide (Fig. 2.4A). This result independently confirms the FT-ICR MS data that COS BTPC is phosphorylated *in vivo* at Ser⁴⁵¹. In contrast, anti-pSer⁸⁷⁹ failed to detect corresponding BTPC polypeptides on SDS-PAGE immunoblots. Although, this does not rule out the possibility that this site may be phosphorylated in other tissues and/or stress conditions, it indicates it is not *in vivo* phosphorylated in the BTPC of developing COS endosperm. FT-ICR MS data

indicates that Thr⁴ of COS BTPC is an *in vivo* N-terminal phosphorylation site. This is consistent with the phosphorylation predication software NetPhos (<http://www.cbs.dtu.dk/services/NetPhos/>) which predicts Thr⁴ to have a high probability of phosphorylation (0.833) (eg. relative to Thr⁵ (0.244)) (Appendix A).

Monitoring Ser⁴⁵¹ phosphorylation status throughout COS development and following COS depodding

Anti-pSer⁴⁵¹ immunoblots were used to monitor changes in Ser⁴⁵¹ phosphorylation status of BTPC during COS development and in response to the removal of photosynthate supply. These results are interpreted in comparison with those previously obtained using phosphosite-specific antibodies towards the single regulatory N-terminal Ser¹¹ phosphorylation site of the PTPC subunit of Class-1 PEPC from developing COS [39,48] as well as the established Ser⁴²⁵ phosphorylation site of COS BTPC [71]. An affinity-purified antibody raised against recombinant COS BTPC (anti-BTPC) detects BTPC polypeptides independent of their phosphorylation status and allowed for normalization of total BTPC on immunoblots [71,73]. Parallel anti-pSer⁴⁵¹ and anti-BTPC immunoblots of co-IP'd samples from four stages of COS endosperm revealed a distinct developmental pattern in which phosphorylation at Ser⁴⁵¹ decreased from stage III-V, increased again at stage VII, and then rapidly decreased by stage IX (Fig. 2.4B and Appendix B). In COS endosperm, developmental stage III marks rapid cell expansion, stage V–VII represent the major phases of oil and protein accumulation, and at stage IX the seed is almost mature, has lost vascular connection with the parent plant, and has begun to desiccate [25,87,88]. The developmental profile of PTPC Ser¹¹ phosphorylation was somewhat similar to that of BTPCs Ser⁴⁵¹, with phosphorylation

peaking at stage VII, the maximal stage of oil production, and declining by stage IX [39,48], the decrease in phosphorylation at Ser⁴⁵¹ from stage III-V, however, is not seen in PTPC Ser¹¹ phosphorylation. By contrast, the Ser⁴²⁵ phosphorylation status of BTPC continuously increased throughout development becoming maximal in stage IX developing COS [71]. A depodding treatment, which eliminates photosynthate import, had no apparent effect on Ser⁴⁵¹ phosphorylation after 4 days (Fig. 2.4C). This contrasts with Ser⁴²⁵ phosphorylation of COS BTPC which 4 days after depodding displayed a significant increase [71]. In contrast, the regulatory phosphorylation at Ser¹¹ is dependent upon the presence of imported photosynthate such that depodding or prolonged darkness caused the complete dephosphorylation and subsequent monoubiquitination of Class-1 PTPC after 48 h (concomitant with disappearance of PPCK activity) [39,48]. Therefore, like Ser⁴²⁵, phosphorylation of BTPC at Ser⁴⁵¹ appears to be regulated independently of corresponding COS PTPC. However, differences in their developmental profile and also in the nature of their phosphorylation site motifs suggest that *in vivo* Ser⁴⁵¹ and Ser⁴²⁵ phosphorylation status of BTPC are likely controlled by different kinases/phosphatases.

Characterization of phosphomimetic mutants suggests that Ser⁴⁵¹ phosphorylation inhibits BTPC within a Class-2 PEPC complex

Numerous lines of evidence indicate that green algal and vascular plant BTPC subunits only exist *in vivo* as part of the heteromeric Class-2 PEPC complex [12,58,67,74]. For example heterologously expressed COS BTPC aggregate and precipitate upon purification on their own but spontaneously rearrange to form stable Class-2 PEPC complexes when mixed with a Class-1 PEPC [73]. Within Class-2 PEPC, BTPC functions as both a catalytic and regulatory subunit [71,73]. Kinetic analysis of Class-2

PEPC using catalytically inactive mutant subunits showed that the PTPC subunits constitute allosterically sensitive, low V_{max} and low $K_m(PEP)$ catalytic sites, whereas the BTPC subunits constitute allosterically insensitive, high V_{max} and high $K_m(PEP)$ catalytic sites [71,73]. A phosphomimetic mutant of COS BTPC (RcPPC4_S425D) was mixed with a catalytically inactive *Arabidopsis* PTPC subunit (AtPPC3_R644A) and kinetics of the resultant Class-2 PEPC were compared with kinetics of a parallel recombinant Class-2 PEPC containing wild-type COSBTPC [71]. This strategy avoided the complicating effect of having simultaneously active PTPC and BTPC subunits and was clearly able to show that the S425D BTPC mutation was inhibitory, causing an increase in both its $K_m(PEP)$ and sensitivity to feedback inhibition by malate and Asp [71]. The same strategy was used here to determine the effect of phosphomimetic mutations at both Thr⁴ and Ser⁴⁵¹. Site-directed mutagenesis was performed to create the mutant subunits RcPPC4_T4D and RcPPC4_S541D. A third double BTPC mutant was also created which contained both the S425D and S451D mutations. *E. coli* lysates containing the mutant BTPCs were combined with the inactive PTPC subunit AtPPC3_R644A to form mutant Class-2 PEPCs. Each lysates containing Class-2 PEPC was then purified to homogeneity by nickel affinity and gel filtration FPLC as previously described (Fig. 2.5 and Appendix A) [71,73]. The mutations did not appear to affect binding between the PTPC and BTPC subunits as the complexes all eluted off the final gel filtration column as stable hetero-octamers of ~900 kDa.

Kinetic properties of the three phosphomimetic mutants were compared to the wild type BTPC and previously described RcPPC4_S425D BTPC subunits [71]. The PEP substrate saturation kinetics at both optimal and suboptimal pH, (8 and 7.3 respectively),

are shown in Table 2.1. The S451D mutation caused an approximately 2.5-3 fold increase in the $K_m(PEP)$ compared to wild type at both pH levels. This is very similar to the results obtained with the S425D mutation [71]. The double S425D+S451D mutant appeared to be less inhibited than either of the single mutations. By contrast, T4D mutation did not affect BTPC's $K_m(PEP)$ value, but elicited a relatively minor 1.4-fold increase in this parameter at pH 7.3. It does not appear that any of the mutations had a significant influences on the enzyme's V_{max} . The sensitivity to allosteric effectors was also analyzed (Fig. 2.6). Each mutant was tested against various PEPC allosteric effectors (2 mM each) at pH 7.0 and subsaturating (1 mM) PEP. The effectors included the PTPC inhibitors glutamate, malate, aspartate and the PTPC activators glucose-1-phosphate, fructose-6-phosphate, glucose-6-phosphate and glycerol-3-phosphate. Malate and aspartate were the only two metabolites that appeared to have a significant effect on the activity of the BTPC subunits (Fig. 2.6). The S451D mutation caused an approximately 2-fold decrease in the I_{50} (malate) and I_{50} (Asp) values under these conditions. This result was similar to the effect of the S425D mutation [71], whereas the double S425D+S451D mutant showed a less pronounced increase in sensitivity to feedback inhibition than either single mutation. By contrast the T4D mutation had no significant effect on the sensitivity to feedback inhibition by Asp or malate.

The effect of pH on the activity of the S451D and T4D BTPC mutants was determined at saturating (15 mM) and subsaturating PEP (2 mM). No differences in pH dependence of the two phosphomimetic mutants were noted at either PEP concentration (Fig. 2.7). Altogether, the S451D mutation appears to be inhibitory in nature, causing an increase in the enzyme's $K_m(PEP)$ and sensitivity to feedback inhibition by malate and

Asp. This provides strong evidence that the introduction of the negative charges associated with a phosphate group to the Ser⁴⁵¹ residue (i.e. *in vivo* phosphorylation) would have a similar inhibitory impact. Ultimately, this conclusion needs to be experimentally verified by analysis of the addition or removal of a phosphate group from Ser⁴⁵¹ of COS BTPC. As native COS BTPC cannot be purified intact due to proteolysis [7], work is underway to identify either an endogenous or exogenous kinase that is capable of site-specific phosphorylation at this residue.

Remarkably, the inhibitory effects of the S451D mutation appear to be quite similar to the previously described S425D mutation [71]. The fact that there are two regulatory phosphorylation sites within close proximity clearly implicates the intrinsically disordered region as a site of regulatory control for BTPC. An unexpected finding was that the BTPC double mutant S425D+S451D was less inhibited than either or the single mutants. However, as no structural data is available for BTPCs disordered region, it is difficult to predict what interaction between these two residues may occur to possibly account for this attenuation of inhibition. Based on earlier findings using P_i-affinity PAGE [72], it is clear that BTPC from developing COS endosperm exists in a high state of multi-site phosphorylation. Combined with their developmental patterns and response to photosynthate limitation, it appears that there would be considerable overlap between the occurrences of the Ser⁴²⁵ and Ser⁴⁵¹ phosphorylation sites. Clearly, more research is needed to provide a rationale for multisite phosphorylation in this region as a new mechanism of PEPC enzyme control. In this regard, it will be of great interest to identify the corresponding kinases and phosphatases that control phosphorylation at these sites as well as to determine the nature of the upstream signaling pathway.

2.5 Conclusion

Within the developing COS endosperm there exist two distinct subunits and isoforms of PEPC. Class-1 PEPC is controlled by phosphorylation of its PTPC subunits at Ser¹¹ to be in tune with the presence of imported photosynthate from the leaves and the developmental stage of the seed. This strongly suggests a role for Class-1 PEPC in regulating carbon metabolism in support of the accumulation of storage compounds in the developing endosperm. The Class-2 PEPC has kinetic properties that would allow it to function as a metabolic overflow mechanism, sustaining flux from PEP to malate when PEP levels were high but Class-1 PEPCs may be largely inactivated by feedback inhibition. In this capacity, BTPC and Class-2 PEPC may allow an increased rate of biosynthesis in the developing seeds. However, verification of this hypothesis requires: (i) further examples of the existence of Class-2 PEPC in similar metabolic environments outside the developing COS endosperm and (ii) the elucidation of mechanisms of control for BTPC that are in line with this proposed physiological role. The current study furthers previous research which proposed multisite phosphorylation as a post-translational mechanism for the control of COS BTPC *in vivo* [71,72]. Both Ser⁴²⁵ and Ser⁴⁵¹ have been shown to be *in vivo* phosphorylation sites whose corresponding phosphomimetic mutations cause inhibition of the BTPC subunits. It is not yet clear how phosphorylation at these sites contributes to the regulation of carbon metabolism *in vivo*, and the discovery of environmental stimuli or cellular conditions that modulate phosphorylation at these sites would thus be a major advancement. Nevertheless, the additional post-translational control mechanisms would allow endosperm PEPC activity to respond more dynamically and rapidly to meet the needs of the cell. Conversely, pThr⁴ does not appear

to play a regulatory role in COS BTPC as suggested by kinetic analysis of the T4D phosphomimetic mutant. Thr⁴ does, however, exist in a FHA binding motif pTXXD known to mediate protein-protein interactions through pThr. Additional work is needed to confirm the role of pThr⁴ in BTPC and its potential role mediating protein-protein interactions in developing COS.

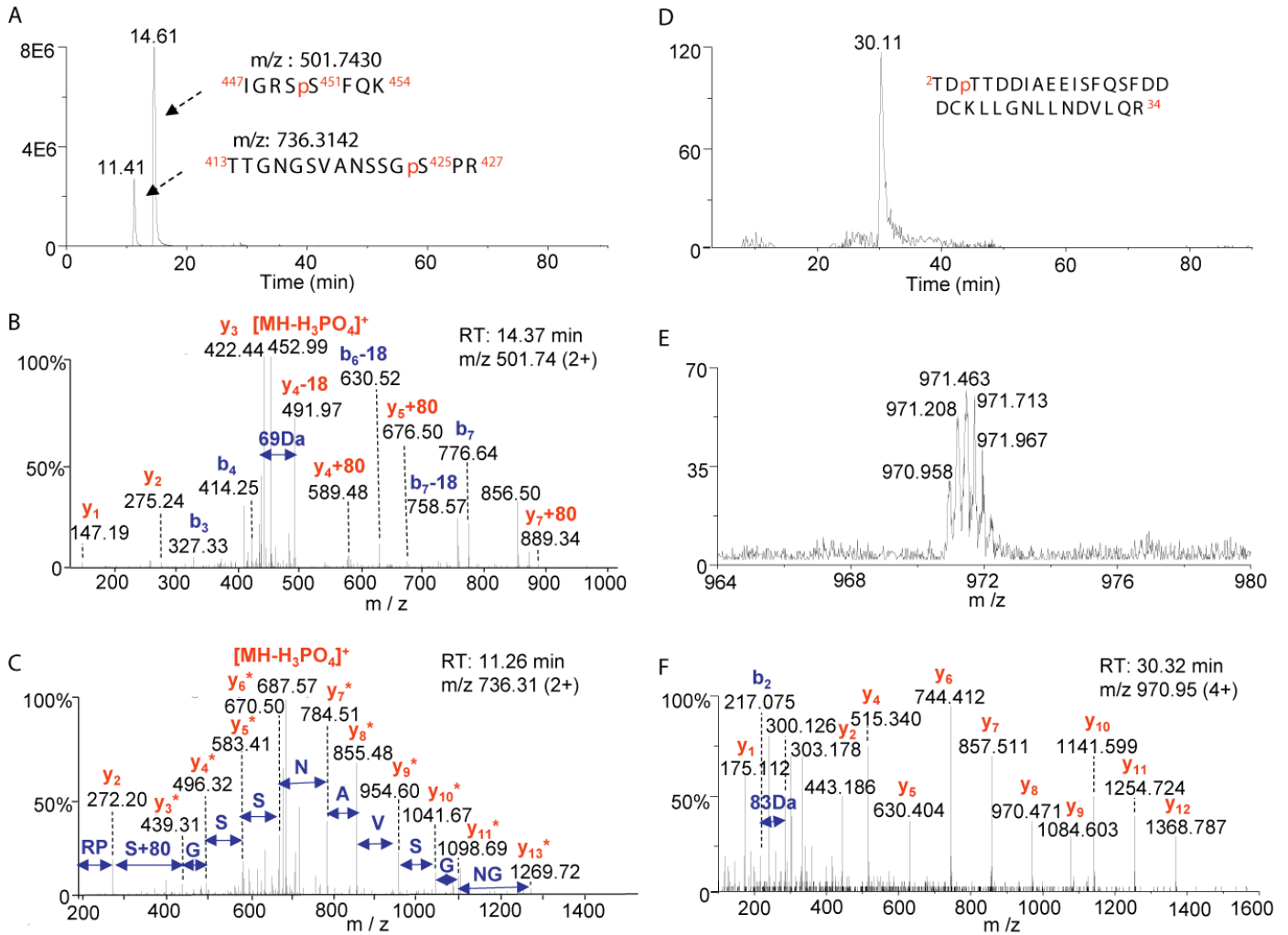


Figure 2.1: COS BTPC MS/MS analysis and phosphorylation site mapping

Ultra Performance Liquid Chromatography (UPLC) LTQ-FT MS/MS identification of the *in vivo* phosphorylation of bacterial-type phosphoenolpyruvate carboxylase. **(A)** The extracted ion chromatograms (XICs) of the phosphopeptide ions at m/z 736.3142 and m/z 501.7430. **(B)** MS/MS spectrum of the doubly-charged ion at m/z 736.31. **(C)** MS/MS spectrum of the doubly-charged ion at m/z 501.74. RT refers to LC retention time. HPLC QqTOF identified a large phosphorylated peptide at site Thr⁴. **(D)** The extracted chromatogram of the phosphopeptide ion at m/z 970.95 indicating position of the Pi groups. **(E)** MS spectrum of the ion shows a charge state of 4+. **(F)** MS/MS spectrum of the quadruply-charged ion at m/z 970.95. RT refers to LC retention time.

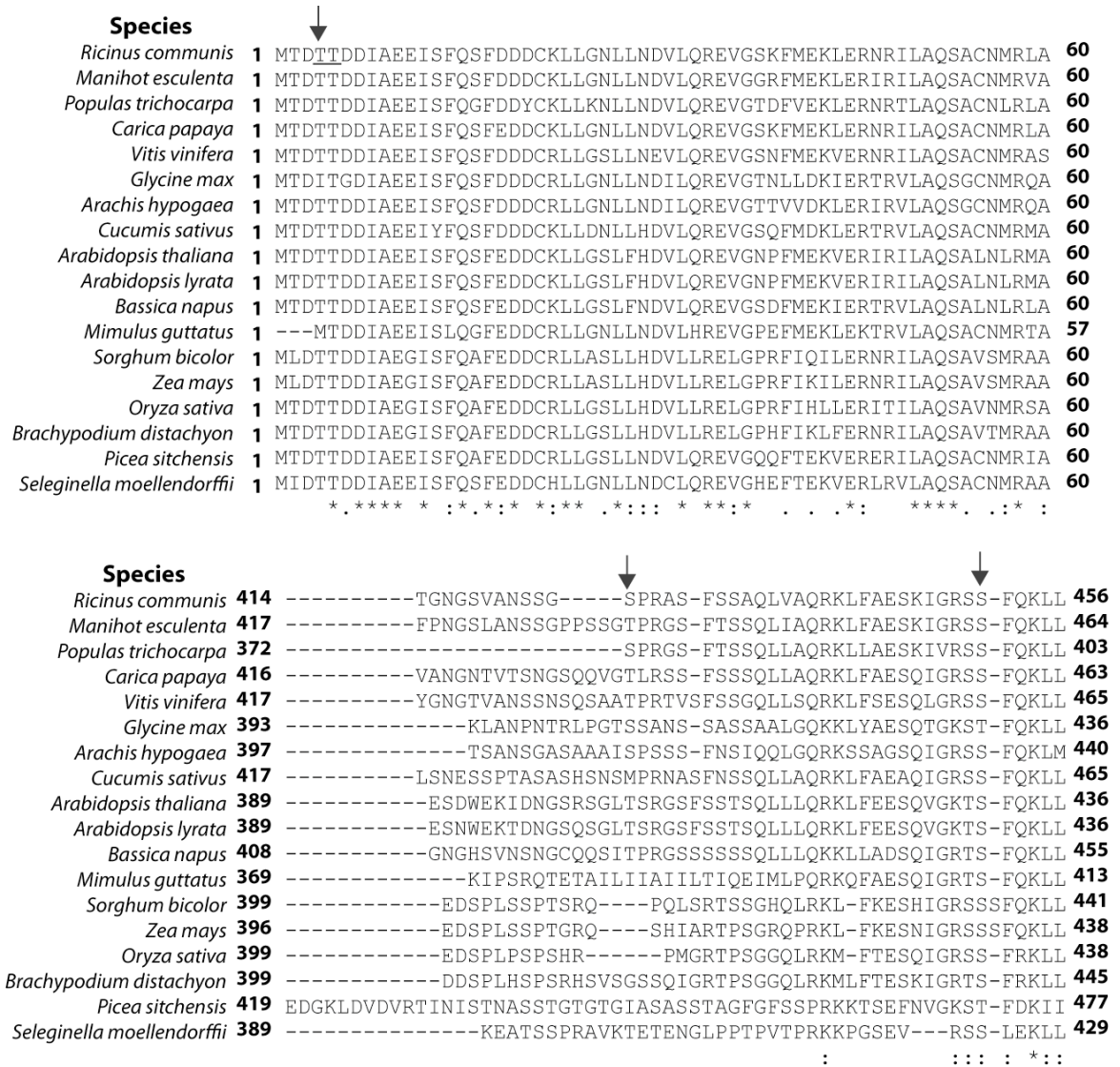


Figure 2.2: Partial alignment of COS BTPC Thr⁴ and Ser⁴⁵¹ domains with other vascular plant BTPCs. Available full length plant BTPC amino acid sequences were aligned using the Toffee program (available online at <http://www.toffee.org/>). Ser⁴²⁵, Ser⁴⁵¹ and Thr⁴ are indicated by the arrows. *, : and . indicate decreasing degrees of conservation. The protein sequences were identified using NCBI's BLAST program and the NCBI (<http://www.ncbi.nlm.nih.gov/>) or Phytozome (www.phytozome.org) databases.

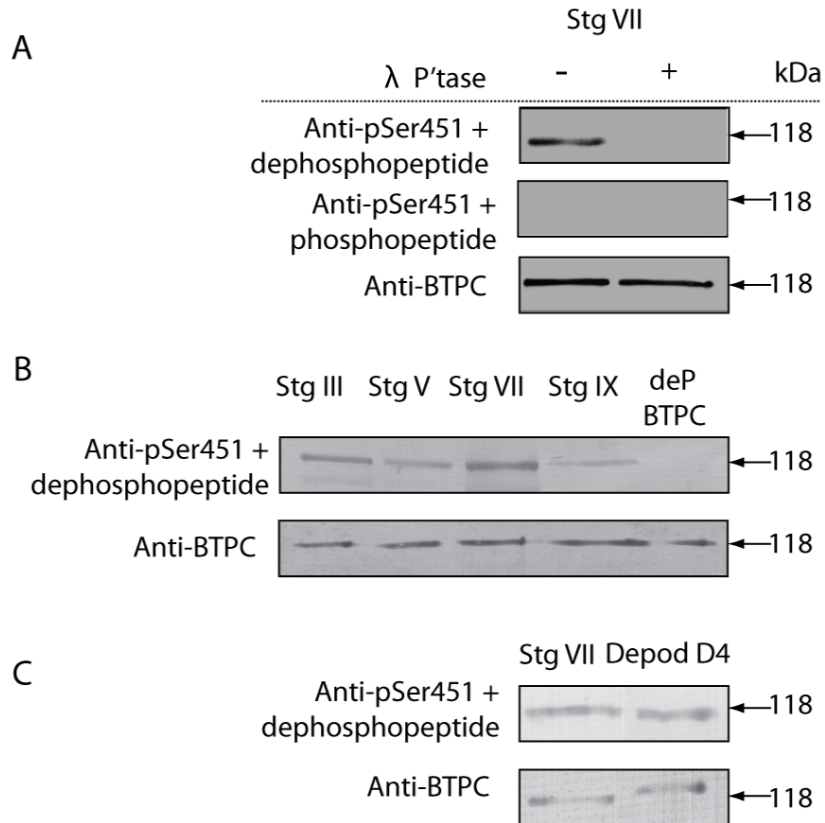


Figure 2.4: ***In vivo* phosphorylation status of Ser⁴⁵¹ in developing COS endosperm**
(A) Co-immunopurified BTPC from stage VII developing endosperm was incubated with (+) and without (-) λ -phosphatase (λ -P'tase). Samples were subjected to SDS-PAGE followed by immunoblotting with anti-BTPC or anti-pSer⁴⁵¹ in the presence of 10 μ g/mL of dephosphopeptide or corresponding phosphopeptide **(B)**. Co-IP COS extracts were loaded based on equal BTPC content, subjected to SDS-PAGE, then immunoblotted with anti-pSer⁴⁵¹ and anti-BTPC. The negative control (deP BTPC) is purified recombinant (dephosphorylated) castor-BTPC expressed in *E. coli*. Biological replicates are shown in Appendix B. **(C)** Co-IP'd extracts from Stage VII developing endosperm harvested at mid-day was used as a standard and compared to stage VII endosperm from intact developing COS that had been depodded for four days.

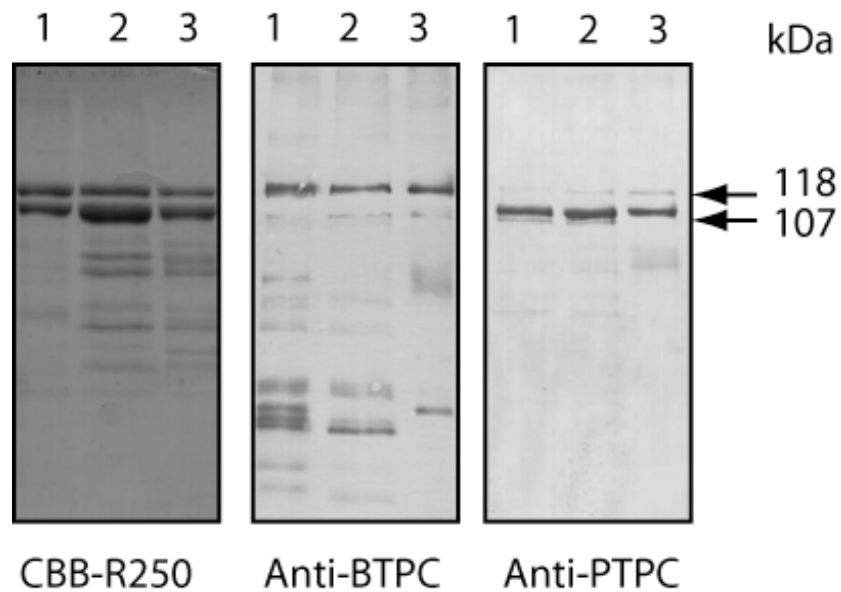


Figure 2.5: **Purification of recombinant Class-2 PEPC mutants** Final preparations of three Class-2 PEPC mutants were subjected to SDS/PAGE followed by Coomassie Brilliant Blue 250 (CBB-R250) staining and immunoblotting with anti-BTPC or anti-PTPC. The lanes were loaded in the following order (PTPC/BTPC): lane 1, AtPPC3_R644A/RcPPC4_T4D; lane 2, AtPPC3_R644A/RcPPC4_S451D; lane 3, AtPPC3_R644A/RcPPC4_S425D-S451D.

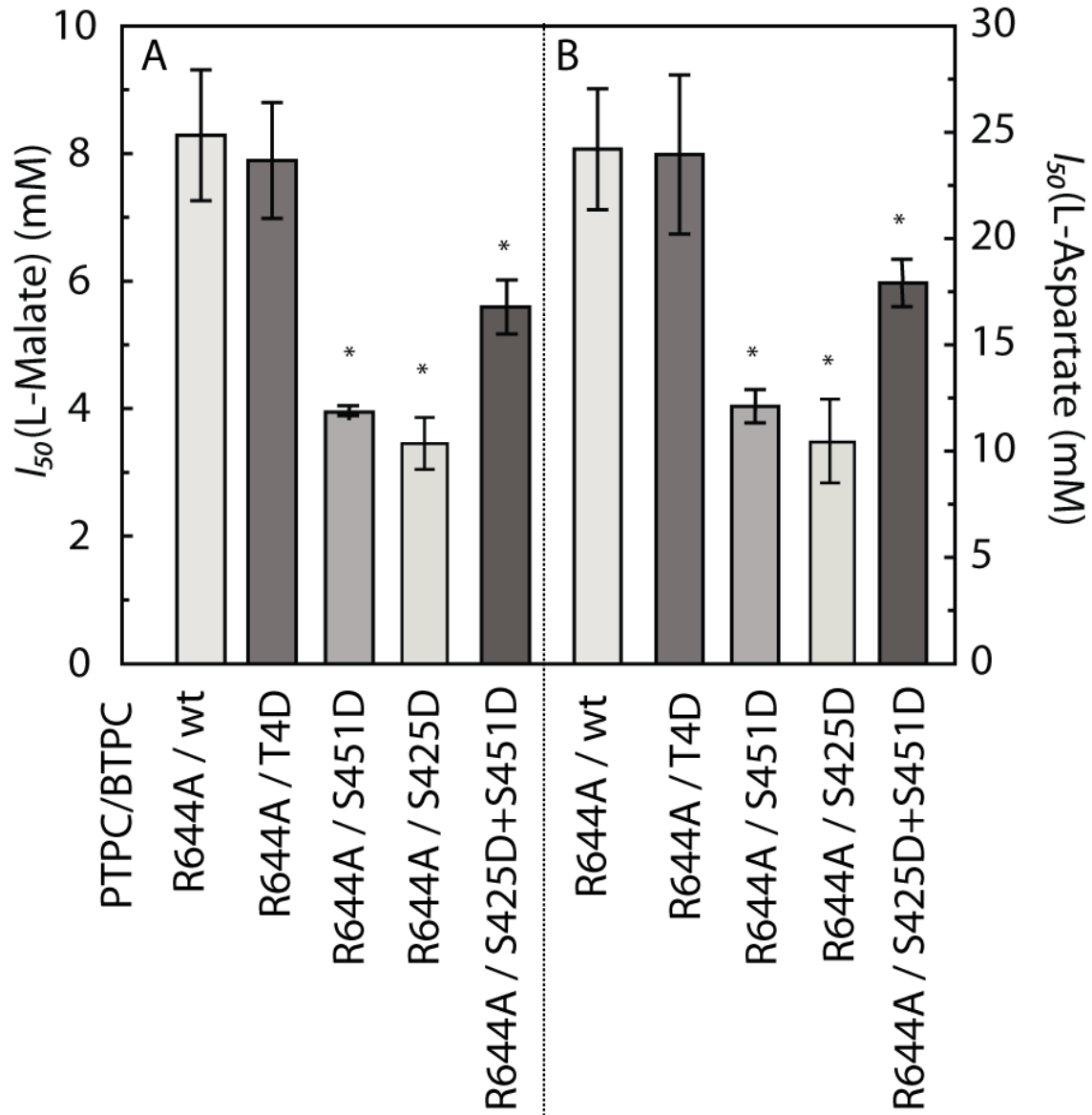


Figure 2.6: **Sensitivity of recombinant Class-2 PEPC mutants to effectors.** (A and B) PEPC activity was determined at pH 7.0 with subsaturating PEP (2 mM) in the presence of increasing concentrations of L-malate and L-aspartate. Shown are the I_{50} (malate) (A) or I_{50} (aspartate) (B) values for several subunit combinations of Class-2 PEPC. The PTPC subunit was an inactive mutant (AtPPC3_R644A). The BTPC subunit was either wild-type (wt)(RcPPC4), or active (RcPPC4_T4D, RcPPC4_S451D, RcPPC4_S425D (data for R644A/S425D are from [71]) and RcPPC4_S425D+S451D) site-directed mutants. All values represent the means \pm S.E.M. of at least four separate determinations. Asterisks denote values are significantly different from R644A/wt ($p < 0.02$).

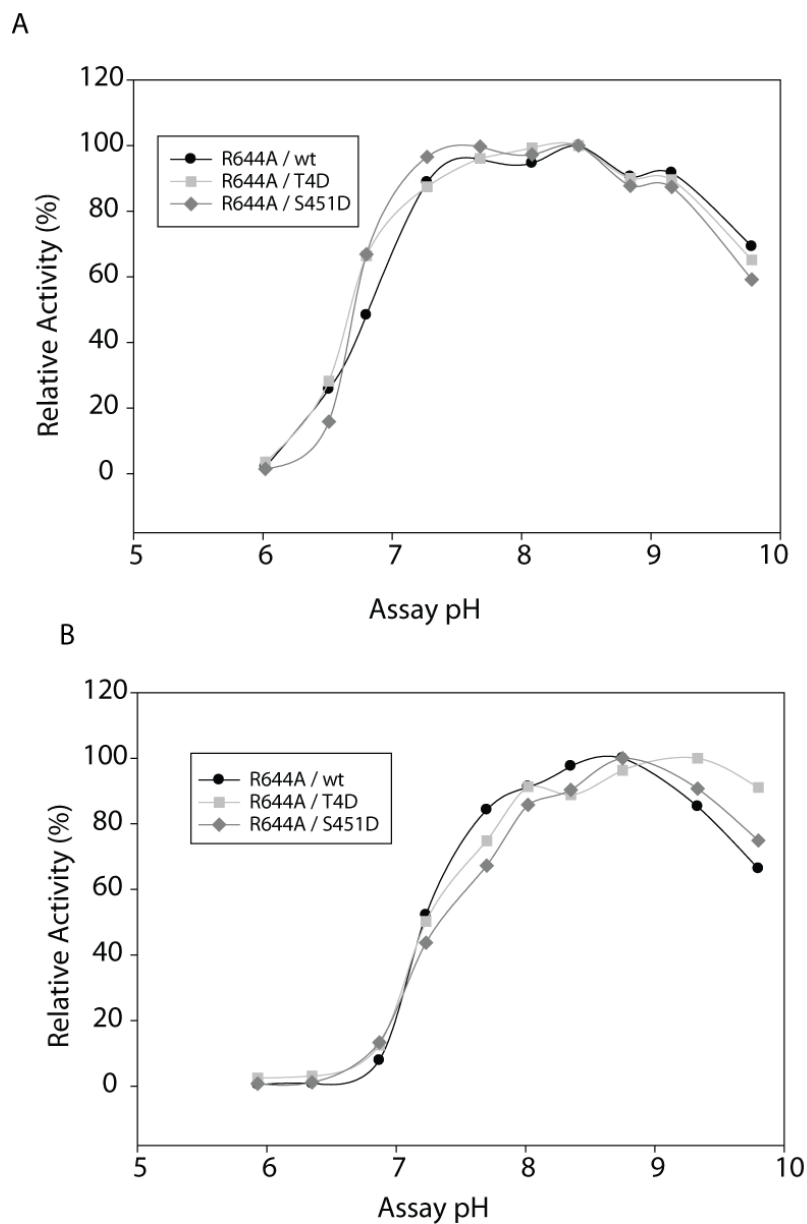


Figure 2.7: **pH activity profile of recombinant Class-2 PEPC mutants.** PEPC activity for R644A / wt, R644A / T4D and R644A / S451D was determined with **(A)** saturating PEP (15 mM) or **(B)** subsaturating PEP (2 mM) at various pH values using a mixture of 50 mM bis-Tris-propane and 50 mM MES as the buffer. All values represent the mean of at least three separate determinations and are reproducible to within $\pm 10\%$ S.E.M. of the mean value.

Table 2.1: PEP saturation kinetics of wild-type and phosphomimetic mutants of heterologously expressed Class-2 PEPC

All values represent the mean of four separate determinations and are reproducible to within $\pm 15\%$ S.E.M. of the mean value.

Class-2 PEPC Isoform	pH 7.3		pH 8.0	
	V_{max} (units•mg ⁻¹)	K_m (PEP) (mM)	V_{max} (units•mg ⁻¹)	K_m (PEP) (mM)
<u>AtPPC3 / RcPPC4</u>				
R644A / wild type	9.4	0.76	11	0.74
R644A / S451D	12.5	2.4	11.7	2.1
R644A / T4D	11.7	1.1	13.8	0.76
R644A / S451D-S425D	10.0	1.6	11.2	0.95

Chapter 3. General Discussion

Work presented in this thesis has furthered our understanding of multisite *in vivo* phosphorylation of Class-2 PEPC's BTPC subunits in developing COS. Initial purification of two distinct classes of PEPC from developing COS not only determined the presence of the Class-2 PEPC, but led to kinetic evaluation deeming the novel Class-2 PEPC heteromeric complex to have a lower affinity for PEP and be less sensitive to allosteric effectors [10]. Subsequent studies on BTPC phospho-sites provided a solid foundation for characterizing the remaining PTMs of COS BTPC.

With the ability to employ protease inhibitors to largely suppress the proteolytic problems first faced when purifying native COS BTPC, co-IP phosphoproteomic studies determined that BTPC was phosphorylated at multiple sites *in vivo* [72]. This represents the first reported case of vascular plant BTPC phosphorylation. LTQ-FT MS/MS of co-IP'd COS BTPC was then used to identify its specific phospho-sites to Thr⁴, Ser⁴²⁵ and Ser⁴⁵¹. Work by Brendan O'Leary on Ser⁴²⁵ provided a useful foundation for studying BTPC phospho-sites [71]. His kinetic studies of S425D phosphomimetic mutants indicated that was found that Ser⁴²⁵ acted as an inhibitory regulator of BTPC catalytic activity when phosphorylated.

This thesis characterized the BTPC phospho-sites Ser⁴⁵¹ and Thr⁴. Ser⁸⁷⁹ was ruled out as *in vivo* phosphorylation sites due to (i) the inability of anti-pSer⁸⁷⁹ to cross-react with native co'IP'd BTPC, despite being specific for its phospho-peptide, and (ii) failure of FT-ICR MS to identify Ser⁸⁷⁹ as a phospho-site. Ser⁴⁵¹ was confirmed as an *in vivo* phospho-site and was found to be phosphorylated in developing COS endosperm in a pattern quite differently than the Ser¹¹ of COS PTPC and Ser⁴²⁵ of BTPC. Ser⁴⁵¹

showed a marked decrease in phosphorylation at stage V followed by an increase at stage VII and another decrease at stage IX (Fig. 2.4B). This pattern along with the fact that depodding does not change phosphorylation status suggests Ser⁴⁵¹ is controlled by a mechanism yet again different from PTPC and now Ser⁴²⁵ in BTPC. In addition, phosphomimetic S451D, demonstrated similar kinetic characteristics to S425D, indicating that Ser⁴⁵¹ phosphorylation functions as a regulatory inhibitor in BTPC. Interestingly, when a double mutant (S425D+S451D) was created sensitivity to allosteric inhibitors and affinity for PEP was intermediate to the wild type and the single mutants. This may be due to some interaction between the two phospho-sites and/or the fact that Asp is not identical to phospho-Ser but further studies are needed to understand this effect.

Unfortunately, attempts with several synthetic Thr⁴ phosphopeptide did not produce any antibodies. However, a phosphomimetic T4D mutant demonstrated that this phosphorylation site is not regulatory. Interestingly, pThr⁴ exists in a FHA binding motif. The sequence surrounding Thr⁴ coincides with the one of the two prominent FHA binding motifs described thus far, pTXXD [83]. This indicates that phosphorylation at this site may play a role in mediating some sort of protein:protein interaction. FHA binding domains are typically found in signal transduction pathways and have been recently found in plants in the KAPP and DDL proteins, involved in receptor kinases and miRNA/siRNA biogenesis, respectively [89,90]. If BTPC pThr⁴ mediates *in vivo* binding of BTPC to an FHA domain containing protein it would be the first record of FHA binding proteins involved in a plant metabolic pathway.

With more known about this novel Class-2 PEPC questions arise regarding its function in COS endosperm. Why does COS endosperm contain two distinct oligomeric isoforms of PEPC? Evaluation of the kinetic properties of recombinant Class-2 PEPC show that the catalytic contribution of its BTPC subunits allows the complex to remain active in the presence of high levels of malate. The estimated malate concentration in developing COS is ~5 mM [24], at this concentration the PTPC containing Class-1 PEPC (whose I_{50} malate is ~0.15 mM) would be completely inhibited. By contrast, BTPC has an I_{50} malate of ~8 mM (Fig. 2.6). BTPC may therefore be acting in response to cytosolic malate concentrations. However, BTPC does have a high K_m (PEP) of around 0.7 mM, so may require relatively high concentrations of PEP to become noticeably active. Class-2 PEPC is then potentially acting as a metabolic overflow mechanism to allow continued flux from PEP to organic acids during periods of rapid biosynthesis when elevated malate concentrations may inhibit Class-1 PEPC. The benefit of having such a mechanism to keep malate concentrations high in the cell may be to increase sink strength and support higher rates of fatty acid and amino acid biosynthesis in developing COS.

Understanding these pathways and more specifically Class-1 and -2 PEPCs may lead to potential sites of control of carbon partitioning in developing seed. This could lead to rational metabolic engineering efforts aimed at increasing crop yield. It may be a promising area to engineer as BTPC is expressed in tissues of high biosynthetic activity such as the developing seed, which could lead to potentially increasing sink storage. It has been previously shown that modifications to PEPC that reduce feedback inhibition are more effective than simple overexpression [18,44,91,92]. BTPC is already

desensitized to feedback inhibition, making it an attractive candidate for PEPC metabolic engineering in vascular plants.

Another promising area would be to further address the PTMs of BTPC, by creating Ser to Ala mutants that cannot be phosphorylated at the regulatory sites (Ser⁴²⁵ and Ser⁴⁵¹). This may provide more information as to how the two phosphorylation sites are interacting with each other and could lead to furthering the information presented with the double phosphomimetic mutant (S425D+S451D). Finally, searching for an FHA-domain containing binding partner of the pThr⁴ site would give insight into a possible BTPC protein interactome. This could be approached by eluting clarified COS extracts through a pThr⁴ peptide affinity column to search for endogenous protein interactors. Parallel elution through a control dephosphorylated Thr⁴ peptide column would be necessary to confirm pThr⁴ dependence of any putative interactors. In addition, despite the fact that BTPC's Ser⁸⁷⁹ is not phosphorylated in developing COS endosperm future work needs to consider its possible phosphorylation in BTPC of other castor tissues or plant species.

Finally, with three phosphorylation sites identified in COS BTPC it will be crucial to investigate the kinases and phosphatases (and related signaling pathways) responsible for regulating site-specific BTPC phosphorylation. Each BTPC phosphorylation site also appears to exist in very different kinase recognition motifs (acidic (Thr⁴), proline directed (Ser⁴²⁵) and basophilic (Ser⁴⁵¹)) suggesting that each site may in fact be regulated by different kinases and phosphatases.

References

- 1 Chollet, R., Vidal, J. and O'Leary, M. (1996) Phosphoenolpyruvate carboxylase: A ubiquitous, highly regulated enzyme in plants. *Annu. Rev. Plant Phys. Plant Mol. Biol.* **47**, 273-298
- 2 Izui, K., Matsumura, H., Furumoto, T. and Kai, Y. (2004) Phosphoenolpyruvate carboxylase: A new era of structural biology. *Ann. Rev. Plant Biol.* **55**, 69-84
- 3 Sanchez, R. and Cejudo, F. J. (2003) Identification and expression analysis of a gene encoding a bacterial-type phosphoenolpyruvate carboxylase from arabidopsis and rice. *Plant Physiol.* **132**, 949-957
- 4 Sullivan, S., Jenkins, G. I. and Nimmo, H. G. (2004) Roots, cycles and leaves. expression of the phosphoenolpyruvate carboxylase kinase gene family in soybean. *Plant Physiol.* **135**, 2078-2087
- 5 Mamedov, T. G., Moellering, E. R. and Chollet, R. (2005) Identification and expression analysis of two inorganic C- and N-responsive genes encoding novel and distinct molecular forms of eukaryotic phosphoenolpyruvate carboxylase in the green microalga *Chlamydomonas reinhardtii*. *Plant J.* **42**, 832-843
- 6 Igawa, T., Fujiwara, M., Tanaka, I., Fukao, Y. and Yanagawa, Y. (2010) Characterization of bacterial-type phosphoenolpyruvate carboxylase expressed in male gametophyte of higher plants. *BMC Plant Biol.* **10**, 200
- 7 Gennidakis, S., Rao, S., Greenham, K., Uhrig, R. G., O'Leary, B., Snedden, W. S., Lu, C. and Plaxton, W. C. (2007) Bacterial- and plant-type phosphoenolpyruvate carboxylase polypeptides interact in the hetero-oligomeric class-2 PEPC complex of developing castor oil seeds. *Plant J.* **52**, 839-849
- 8 Kai, Y., Matsumura, H. and Izui, K. (2003) Phosphoenolpyruvate carboxylase: Three-dimensional structure and molecular mechanisms. *Arch. Biochem. Biophys.* **414**, 170-179
- 9 Ting, I. P. and Osmond, C. B. (1973) Photosynthetic phosphoenolpyruvate carboxylases: Characteristics of alloenzymes from leaves of C3 and C1 plants. *Plant Physiol.* **51**, 439-447
- 10 Blonde, J. and Plaxton, W. C. (2003) Structural and kinetic properties of high and low molecular mass phosphoenolpyruvate carboxylase isoforms from the endosperm of developing castor oilseeds. *J. Biol. Chem.* **278**, 11867-11873
- 11 Rivoal, J., Plaxton, W. C. and Turpin, D. (1998) Purification and characterization of high- and low-molecular-mass isoforms of phosphoenolpyruvate carboxylase from *Chlamydomonas reinhardtii*. *Biochem J.* **331**, 201-209
- 12 Rivoal, J., Trzos, S., Gage, D., Plaxton, W. C. and Turpin, D. (2001) Two unrelated phosphoenolpyruvate carboxylase polypeptides physically interact in the high molecular

mass isoforms of this enzyme in the unicellular green alga *Selenastrum minutum*. J. Biol. Chem. **276**, 12588-12601

- 13 Vidal, J. and Chollet, R. (1997) Regulatory phosphorylation of C-4 PEP carboxylase. Trends Plant Sci. **2**, 230-237
- 14 Svensson, P., Bläsing, O. E. and Westhoff, P. (2003) Evolution of C4 phospho*enol*pyruvate carboxylase. Arch Biochem Biophys. **414**, 180-188
- 15 Nimmo, H. G. (2000) The regulation of phospho*enol*pyruvate carboxylase in CAM plants. Trends Plant Sci. **5**, 75-80
- 16 Hibberd, J. M. and Covshoff, S. (2010) The regulation of gene expression required for C-4 photosynthesis. Annu. Rev. Plant Biol. **61**, 181-207
- 17 O'Leary, B., Park, J. and Plaxton, W. C. (2011) The remarkable diversity of plant PEPC (phospho*enol*pyruvate carboxylase): recent insights into the physiological functions and post-translational controls of non-photosynthetic PEPCs. Biochem. J. **436**, 15-34
- 18 Rolletschek, H., Borisjuk, L., Radchuk, R., Miranda, M., Heim, U., Wobus, U. and Weber, H. (2004) Seed-specific expression of a bacterial phospho*enol*pyruvate carboxylase in *Vicia narbonensis* increases protein content and improves carbon economy. Plant Biotech. J. **2**, 211-219
- 19 Radchuk, R., Radchuk, V., Goetz, K., Weichert, H., Richter, A., Emery, R. J. N., Weschke, W. and Weber, H. (2007) Ectopic expression of phospho*enol*pyruvate carboxylase in *Vicia narbonensis* seeds: Effects of improved nutrient status on seed maturation and transcriptional regulatory networks. Plant J. **51**, 819-839
- 20 Weber, H., Borisjuk, L. and Wobus, U. (2005) Molecular physiology of legume seed development. Ann. Rev. Plant Biol. **56**, 253-279
- 21 Rawsthorne, S. (2002) Carbon flux and fatty acid synthesis in plants. Prog. Lipid Res. **41**, 182-196
- 22 Baud, S. and Lepiniec, L. (2010) Physiological and developmental regulation of seed oil production. Prog. Lipid Res. **49**, 235-249
- 23 Pleite, R., Pike, M. J., Garces, R., Martinez-Force, E. and Rawsthorne, S. (2005) The sources of carbon and reducing power for fatty acid synthesis in the heterotrophic plastids of developing sunflower (*Helianthus annuus* L.) embryos. J. Exp. Bot. **56**, 1297-1303
- 24 Smith, R. G., Gauthier, D. A., Dennis, D. T. and Turpin, D. H. (1992) Malate- and pyruvate-dependent fatty acid synthesis in leucoplasts from developing castor endosperm. Plant Physiol. **98**, 1233-1238

- 25 Sangwan, R. S., Singh, N. and Plaxton, W. C. (1992) Phosphoenolpyruvate carboxylase activity and concentration in the endosperm of developing and germinating castor oil seeds. *Plant Physiol.* **99**, 445-449
- 26 Shearer, H. L., Turpin, D. H. and Dennis, D. T. (2004) Characterization of NADP-dependent malic enzyme from developing castor oil seed endosperm. *Arch. Biochem. Biophys.* **429**, 134-144
- 27 Eastmond, P. J., Dennis, D. T. and Rawsthorne, S. (1997) Evidence that a Malate/Inorganic phosphate exchange translocator imports carbon across the leucoplast envelope for fatty acid synthesis in developing castor seed endosperm. *Plant Physiol.* **114**, 851-856
- 28 Alonso, A. P., Goffman, F. D., Ohlrogge, J. B. and Shachar-Hill, Y. (2007) Carbon conversion efficiency and central metabolic fluxes in developing sunflower (*Helianthus annuus* L.) embryos. *Plant J.* **52**, 296-308
- 29 Alonso, A. P., Dale, V. L. and Shachar-Hill, Y. (2010) Understanding fatty acid synthesis in developing maize embryos using metabolic flux analysis. *Metab. Eng.* **12**, 488-497.
- 30 Chan, A. P., Crabtree, J., Zhao, Q., Lorenzi, H., Orvis, J., Puiu, D., Melake-Berhan, A., Jones, K. M., Redman, J., Chen, G., Cahoon, E. B., Gedil, M., Stanke, M., Haas, B. J., Wortman, J. R., Fraser-Liggett, C., Ravel, J. and Rabinowicz, P. D. (2010) Draft genome sequence of the oilseed species *Ricinus communis*. *Nat. Biotech.* **28**, 951-956
- 31 Buchanan, B., Guissem, W. and Jones, R. L. (2000) Biochemistry and molecular biology of plants. *In American Society of Plant Physiologists.*
- 32 Eastmond, J. P. and Graham, I. A. (2001) Re-examining the role of the glyoxylate cycle in oilseeds. *Trends in Plant Science.* **6**, 72
- 33 Law, R. D. and Plaxton, W. C. (1995) Purification and characterization of a novel phosphoenolpyruvate carboxylase from banana fruit. *Biochem. J.* **307**, 807-816
- 34 Moraes, T. F. and Plaxton, W. C. (2000) Purification and characterization of phosphoenolpyruvate carboxylase from *Brassica napus* (rapeseed) suspension cell cultures. *Eur J Biochem.* **267**, 4465-4476
- 35 Nimmo, H. (2003) Control of the phosphorylation of phosphoenolpyruvate carboxylase in higher plants. *Arch. Biochem. Biophys.* **414**, 189-196
- 36 Nimmo, H. G. (2006) Control of phosphoenolpyruvate carboxylase in plants. In *Control of Primary Metabolism in Plants* (Plaxton, W. C. and McManus, M. T., eds.), pp. 219-233, Blackwell Publishing, Oxford, UK
- 37 Li, B. and Chollet, R. (1994) Salt induction and the partial Purification/characterization of phosphoenolpyruvate carboxylase protein-serine kinase from an inducible crassulacean-acid-metabolism (CAM) plant, *Mesembryanthemum-crystallinum* L. *Arch. Biochem. Biophys.* **314**, 247-254

- 38 Wang, Y. H. and Chollet, R. (1993) Partial purification and characterization of phosphoenolpyruvate carboxylase protein-serine kinase from illuminated maize leaves. *Arch. Biochem. Biophys.* **304**, 496-502
- 39 Murmu, J. and Plaxton, W. C. (2007) Phosphoenolpyruvate carboxylase protein kinase from developing castor oil seeds: Partial purification, characterization, and reversible control by photosynthate supply. *Planta.* **226**, 1299-1310
- 40 Taybi, T., Patil, S., Chollet, R. and J.C. Cushman. (2000) A minimal serine/threonine protein kinase circadianly regulates phosphoenolpyruvate carboxylase activity in crassulacean acid metabolism-induced leaves of the common ice plant. *Plant Physiol.* **123**, 1471-1482
- 41 Tsuchida, Y., Furumoto, T., Izumida, A., Hata, S. and Izui, K. (2001) Phosphoenolpyruvate carboxylase kinase involved in C-4 photosynthesis in *Flaveria trinervia*: CDNA cloning and characterization. *FEBS Lett.* **507**, 318-322
- 42 Monreal, J. A., Lopez-Baena, F. J., Vidal, J., Echevarria, C. and Garcia-Maurino, S. (2007) Effect of LiCl on phosphoenolpyruvate carboxylase kinase and the phosphorylation of phosphoenolpyruvate carboxylase in leaf disks and leaves of *Sorghum vulgare*. *Planta.* **225**, 801-812
- 43 Monreal, J. A., McLoughlin, F., Echevarria, C., Garcia-Maurino, S. and Testerink, C. (2010) Phosphoenolpyruvate carboxylase from C-4 leaves is selectively targeted for inhibition by anionic phospholipids. *Plant Physiol.* **152**, 634-638
- 44 Fukayama, H., Tamai, T., Taniguchi, Y., Sullivan, S., Miyao, M. and Nimmo, H. G. (2006) Characterization and functional analysis of phosphoenolpyruvate carboxylase kinase genes in rice. *Plant J.* **47**, 258-268
- 45 Feria, A., Alvarez, R., Cochereau, L., Vidal, J., Garcia-Maurino, S. and Echevarria, C. (2008) Regulation of phosphoenolpyruvate carboxylase phosphorylation by metabolites and abscisic acid during the development and germination of barley seeds. *Plant Physiol.* **148**, 761-774
- 46 Chen, Z. H., Jenkins, G. I. and Nimmo, H. G. (2008) pH and carbon supply control the expression of phosphoenolpyruvate carboxylase kinase genes in *Arabidopsis thaliana*. *Plant, Cell Environ.* **31(12)**, 1844-1850
- 47 Shenton, M., Fontaine, V., Hartwell, J., Marsh, J. T., Jenkins, G. I. and Nimmo, H. G. (2006) Distinct patterns of control and expression amongst members of the PEP carboxylase kinase gene family in C4 plants. *Plant J.* **48**, 45-53
- 48 Tripodi, K., Turner, W., Gennidakis, S. and Plaxton, W. C. (2005) *In vivo* regulatory phosphorylation of novel phosphoenolpyruvate carboxylase isoforms in endosperm of developing castor oil seeds. *Plant Physiol.* **139**, 969-978

- 49 Xu, W., Zhou, Y. and Chollet, R. (2003) Identification and expression of a soybean nodule-enhanced PEP-carboxylase kinase gene (NE-PpcK) that shows striking up-/down-regulation *in vivo*. *Plant J.* **34**, 441-452
- 50 Xu, W., Sato, S. J., Clemente, T. E. and Chollet, R. (2007) The PEP-carboxylase kinase gene family in *glycine max* (*GmPpcK1-4*): An in-depth molecular analysis with nodulated, non-transgenic and transgenic plants. *Plant J.* **49**, 910-923
- 51 Hartwell, J., Gill, A., Nimmo, G. A., Wilkins, M. B., Jenkins, G. I. and Nimmo, H. G. (1999) Phosphoenolpyruvate carboxylase kinase is a novel protein kinase regulated at the level of expression. *The Plant Journal.* **20**, 333-342
- 52 Dong, L., Masuda, T., Kawamura, T., Hata, S. and Izui, K. (1998) Cloning, expression, and characterization of a root-form phosphoenolpyruvate carboxylase from *Zea mays*: Comparison with the C4-form enzyme. *Plant Cell Phys.* **39**, 865-873
- 53 Law, R. D. and Plaxton, W. C. (1997) Regulatory phosphorylation of banana fruit phosphoenolpyruvate carboxylase by a copurifying phosphoenolpyruvate carboxylase-kinase. *Eur. J. Biochem.* **247**, 642-651
- 54 Saze, H., Ueno, Y., Hisabori, T., Hayashi, H. and Izui, K. (2001) Thioredoxin-mediated reductive activation of a protein kinase for the regulatory phosphorylation of C4-form phosphoenolpyruvate carboxylase from maize. *Plant Cell Physiol.* **42**, 1295-1302
- 55 Nimmo, G. A., Wilkins, M. B. and Nimmo, H. G. (2001) Partial purification and characterization of a protein inhibitor of phosphoenolpyruvate carboxylase kinase. *Planta.* **213**, 250-257
- 56 Plaxton, W. C. and Podestá, F. E. (2006) The functional organization and control of plant respiration. *Crit. Rev. Plant Sci.* **25**, 159-198
- 57 Chang, I., Curran, A., Woolsey, R., Quilici, D., Cushman, J. C., Mittler, R., Harmon, A. and Harper, J. F. (2009) Proteomic profiling of tandem affinity purified 14-3-3 protein complexes in *Arabidopsis thaliana*. *Proteomics.* **9**, 2967-2985
- 58 Gregory, A. L., Hurley, B. A., Tran, H. T., Valentine, A. J., She, Y., Knowles, V. L. and Plaxton, W. C. (2009) *In vivo* regulatory phosphorylation of the phosphoenolpyruvate carboxylase AtPPC1 in phosphate-starved *Arabidopsis thaliana*. *Biochem J.* **420**, 57-65
- 59 Agetsuma, M., Furumoto, T., Yanagisawa, S. and Izui, K. (2005) The ubiquitin-proteasome pathway is involved in rapid degradation of phosphoenolpyruvate carboxylase kinase for C4 photosynthesis. *Plant Cell Physiol.* **46**, 389-398
- 60 Schulz, M., Klockenbring, T., Hunte, C. and Schnabl, H. (1993) Involvement of ubiquitin in phosphoenolpyruvate carboxylase degradation. *Bot. Acta.* **106**, 143-145
- 61 Schnell, J. D. and Hicke, L. (2003) Non-traditional functions of ubiquitin and ubiquitin-binding proteins. *J. Biol. Chem.* **278**, 35857-35860

- 62 Mukhopadhyay, D. and Riezman, H. (2007) Proteasome-independent functions of ubiquitin in endocytosis and signaling. *Science*. **315**, 201-205
- 63 Uhrig, R. G., She, Y., Leach, C. A. and Plaxton, W. W. (2008) Regulatory monoubiquitination of phosphoenolpyruvate carboxylase in germinating castor oil seeds. *J. Biol. Chem.* **283**, 29650-29657
- 64 González, M., Osuna, L., Echevarría, C., Vidal, J. and Cejudo, F. J. (1998) Expression and localization of phosphoenolpyruvate carboxylase in developing and germinating wheat grains. *Plant Physiol.* **116**, 1249-1258
- 65 Nhiri, M., Bakrim, N., Bakrim, N., El Hachimi-Messouak, Z., Echevarria, C. and Vidal, J. (2000) Posttranslational regulation of phosphoenolpyruvate carboxylase during germination of *Sorghum* seeds: Influence of NaCl and -malate. *Plant Sci.* **151**, 29-37
- 66 Osuna, L., Pierre, J., Gonzalez, M., Alvarez, R., Cejudo, F. J., Echevarria, C. and Vidal, J. (1999) Evidence for a slow-turnover form of the Ca²⁺-independent phosphoenolpyruvate carboxylase kinase in the aleurone-endosperm tissue of germinating barley seeds. *Plant Physiol.* **119**, 511-520
- 67 O'Leary, B., Fedoejevs, E., Hill, A., Bettridge, J., Park, J., Rao, S., Leach, C. and Plaxton, W. C. (2011) Tissue-specific expression and post-translational modifications of plant- and bacterial-type phosphoenolpyruvate carboxylase isozymes of the castor oil plant, *Ricinus communis* L. *J. Exp. Bot.* (Accepted, pending revisions)
- 68 Schuller, K. A., Plaxton, W. C. and Turpin, D. H. (1990) Regulation of phosphoenolpyruvate carboxylase from the green alga *Selenastrum minutum*: Properties associated with replenishment of tricarboxylic acid cycle intermediates during ammonium assimilation. *Plant Physiol.* **93**, 1303-1311
- 69 Rivoal, J., Dunford, R., Plaxton, W. C. and Turpin, D. H. (1996) Purification and properties of four phosphoenolpyruvate carboxylase isoforms from the green alga *Selenastrum minutum*: Evidence that association of the 102-kDa catalytic subunit with unrelated polypeptides may modify the physical and kinetic properties of the enzyme. *Arch. Biochem. Biophys.* **332**, 47-57
- 70 Rivoal, J., Turpin, D. and Plaxton, W. C. (2002) *In vitro* phosphorylation of phosphoenolpyruvate carboxylase from the green alga *Selenastrum minutum*. *Plant Cell Physiol.* **43**, 785-792
- 71 O'Leary, B., Rao, S. and Plaxton, W. C. (2011) Phosphorylation of a bacterial-type phosphoenolpyruvate carboxylase at serine-425 provides a further tier of enzyme control in developing castor oil seeds. *Biochem. J.* **433**, 65-74
- 72 Uhrig, R. G., O'Leary, B., Spang, H. E., MacDonald, J. A., She, Y. and Plaxton, W. C. (2008) Coimmunopurification of phosphorylated bacterial- and plant-type phosphoenolpyruvate carboxylases with the plastidial pyruvate dehydrogenase complex from developing castor oil seeds. *Plant Physiol.* **146**, 1346-1357

- 73 O'Leary, B., Rao, S. K., Kim, J. and Plaxton, W. C. (2009) Bacterial-type phosphoenolpyruvate carboxylase (PEPC) functions as a catalytic and regulatory subunit of the novel class-2 PEPC complex of vascular plants. *J. Biol. Chem.* **284**, 24797-24805
- 74 Park, J, Howard, A.S.M., Mullen, R.T. and Plaxton, W.C. (2010) Subcellular localization and *in vivo* interactions of plant- and bacterial-type phosphoenolpyruvate carboxylase isozymes of developing castor seeds. Joint Annual Meeting of the American Society of Plant Biologists/Canadian Society of Plant Physiology, Abstract P02044, Montreal, Quebec, Canada
- 75 Xu, W., Ahmed, S., Moriyama, H. and Chollet, R. (2006) The importance of the strictly conserved, C-terminal glycine residue in phosphoenolpyruvate carboxylase for overall catalysis: Mutagenesis and truncation of gly-961 in the sorghum C4 leaf isoform. *J. Biol. Chem.* **281**, 17238-17245
- 76 Sánchez, R., Flores, A. and Cejudo, F. J. (2006) Arabidopsis phosphoenolpyruvate carboxylase genes encode immunologically unrelated polypeptides and are differentially expressed in response to drought and salt stress. *Planta.* **223**, 901-909
- 77 Gousset-Dupont, A., Lebouteiller, B., Monreal, J., Echevarria, C., Pierre, J. N., Hodges, M. and Vidal, J. (2005) Metabolite and post-translational control of phosphoenolpyruvate carboxylase from leaves and mesophyll cell protoplasts of *Arabidopsis thaliana* . *Plant Sci.* **169**, 1096-1101
- 78 Yu, S., Pan, L., Yang, Q., Chen, M. and Zhang, H. (2010) Identification and expression analysis of the phosphoenolpyruvate carboxylase gene family in peanut (*Arachis hypogaea* L.). *Agricultural Sciences in China.* **9**, 477-487
- 79 Moellering, E. R., Ouyang, Y., Mamedov, T. G. and Chollet, R. (2007) The two divergent PEP-carboxylase catalytic subunits in the green microalga *Chlamydomonas reinhardtii* respond reversibly to inorganic-N supply and co-exist in the high-molecular-mass, hetero-oligomeric class-2 PEPC complex. *FEBS Lett.* **581**, 4871-4876
- 80 Masumoto, C., Miyazawa, S., Ohkawa, H., Fukuda, T., Taniguchi, Y., Murayama, S., Kusano, M., Saito, K., Fukayama, H. and Miyao, M. (2010) Phosphoenolpyruvate carboxylase intrinsically located in the chloroplast of rice plays a crucial role in ammonium assimilation. *Proc. Natl. Acad. Sci. U. S. A.* **107**, 5226-5231
- 81 Plaxton, W. C. (1989) Molecular and immunological characterization of plastid and cytosolic pyruvate kinase isozymes from castor-oil-plant endosperm and leaf. *Eur. J. Biochem.* **181**, 443-451
- 82 Brooks, S. (1992) A simple computer program with statistical tests for the analysis of enzyme kinetics. *Biotechniques.* **13**, 906-911
- 83 Mahajan, A., Yuan, C., Lee, H., Chen, E. S. -, Wu, P. and Tsai, M. (2008) Structure and function of the phosphothreonine-specific FHA domain. *Sci. Signal.* **1**

- 84 O'Leary, M. (1982) Phosphoenolpyruvate carboxylase: An enzymologist's view. *Annu. Rev. Plant Physiol. Plant Mol. Biol.* **33**, 297-315
- 85 Kelley, L. A. and Sternberg, M. J. E. (2009) Protein structure prediction on the web: A case study using the phyre server. *Nat. Protocols.* **4**, 363-371
- 86 Dunker, A. K., Silman, I., Uversky, V. N. and Sussman, J. L. (2008) Function and structure of inherently disordered proteins. *Curr. Opin. Struct. Biol.* **18**, 756-764
- 87 Greenwood, J. S. and Bewley, J. D. (1982) Seed development in *Ricinus communis* (castor bean). I. descriptive morphology *Can. J. Bot.* **60**, 1751-1760
- 88 Simcox, P. D., Garland, W., DeLuca, V., Canvin, D. T. and Dennis, D. T. (1979) Respiratory pathways and fat synthesis in the developing castor oil seed. *Can. J. Bot.* **57(9)**, 1008-1014
- 89 Li, J., Smith, G. P. and Walker, J. C. (1999) Kinase interaction domain of kinase-associated protein phosphatase, a phosphoprotein-binding domain. *Proc. Natl. Acad. Sci. U. S. A.* **96**, 7821-7826
- 90 Yu, B., Bi, L., Zheng, B., Ji, L., Chevalier, D., Agarwal, M., Ramachandran, V., Li, W., Lagrange, T., Walker, J. C. and Chen, X. (2008) The FHA domain proteins DAWDLE in arabidopsis and SNIP1 in humans act in small RNA biogenesis. *Proc. Natl. Acad. Sci. U. S. A.* **105**, 10073-10078
- 91 Miyao, M. and Fukayama, H. (2003) Metabolic consequences of overproduction of phosphoenolpyruvate carboxylase in C3 plants. *Arch. Biochem. Biophys.* **414**, 197-203.
- 92 Rademacher, T., Hausler, R.E., Hirsh H., Zhang, L., Lipka, V., Weier, D., Kreuzaler, F. and Peterhansel, C. (2002) An engineered phosphoenolpyruvate carboxylase redirects carbon and nitrogen flow in transgenic potato plant. *Plant J.* **32**, 25-39
- 93 Plaxton, W.C. and O'Leary, B. (2011) The Central Role of Phosphoenolpyruvate Metabolism in Developing Oilseeds. In Agrawac, G.K. and Rawal R. (Eds.), *Seed Development: OMICS technologies Forward Improvement of Seed Quality and Crop Yield*. Springer

Appendix A

NetPhos phospho-site prediction score and phosphomimetic mutant purifications

Table A1 **NetPhos phospho-site prediction scores for Thr⁴, Thr⁵, Ser⁴⁵¹, Ser⁴²⁵ and Ser⁸⁷⁹ of COS BTPC**

Position	Context	Prediction Score
Thr ⁴	-MTD(pT)TDDI	0.833
Thr ⁵	MTDT(pT)DDIA	0.244
Ser ⁴²⁵	NSSG(pS)PRAS	0.996
Ser ⁴⁵⁰	KIGR(pS)SFQK	0.074
Ser ⁴⁵¹	IGRS(pS)FQKL	0.834
Ser ⁸⁷⁹	TRRKS(pS)TGI	0.997

Table A2 **Purification of recombinant Class-2 PEPC from combined extracts originating from 5 g of AtPPC3_R644A- and 10 g of RcPPC4_T4D-expressing *E. coli***

Step	Activity (units)	Protein (mg)	Specific Activity (units/mg of protein)	Purification (fold)	Yield (%)
Combined extracts	209	3420	0.06	1	100
Ni ²⁺ -affinity FPLC	93.6	115.2	0.81	14	45
Superose-6 FPLC	7.2	1.6	4.5	75	3

Table A3 Purification of recombinant Class-2 PEPC from combined extracts originating from 9 g of AtPPC3_R644A- and 12 g of RcPPC4_S451D-expressing *E. coli*

Step	Activity (units)	Protein (mg)	Specific Activity (units/mg of protein)	Purification (fold)	Yield (%)
Combined extracts	190	356	0.053	1	100
Ni ²⁺ -affinity FPLC	88.3	65.6	1.3	25	46
Superose-6 FPLC	99.2	9.3	10.7	201	52

Table A4 Purification of recombinant Class-2 PEPC from combined extracts originating from 3 g of AtPPC3_R644A- and 10 g of RcPPC4_S425D+S451D-expressing *E. coli*

Step	Activity (units)	Protein (mg)	Specific Activity (units/mg of protein)	Purification (fold)	Yield (%)
Combined extracts	126	1375	0.09	1	100
Ni ²⁺ -affinity FPLC	115	28.6	4	44	91
Superdex-200 FPLC	57.7	4.6	12.4	138	46

Appendix B

Biological Replicates of *in vivo* phosphorylation status of Ser⁴⁵¹ in developing COS endosperm

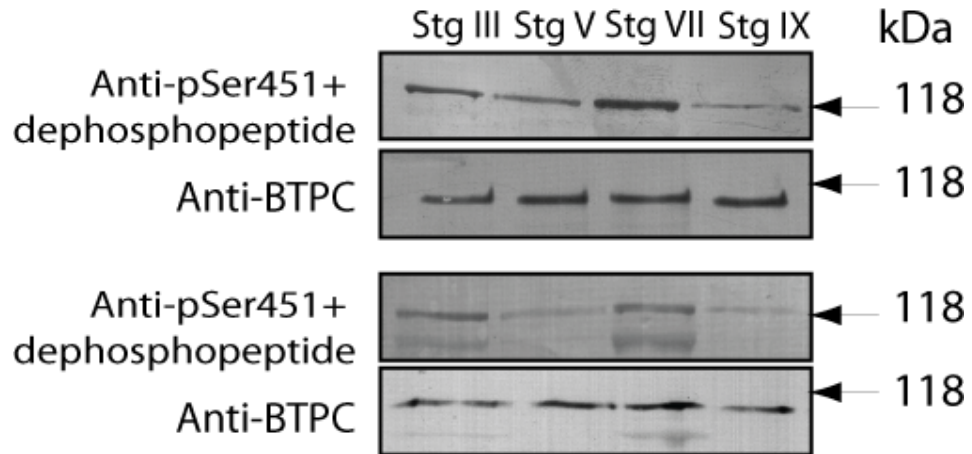


Figure B1: Biological replicates of *in vivo* phosphorylation status of Ser⁴⁵¹ in developing COS endosperm. Co-IP COS extracts were loaded based on equal BTPC content, subjected to SDS-PAGE, then immunoblotted with anti-pSer⁴⁵¹ and anti-BTPC as described in Fig. 2.4. Stages III, V, VII, and IX correspond to the heart-shaped embryo, mid-cotyledon, full cotyledon, and maturation stages of COS developing respectively [71].